UNIVERSIDAD DE SEVILLA

FACULTAD DE ODONTOLOGÍA

DOCTORADO DE CIENCIAS DE LA SALUD

COLOCACIÓN INMEDIATA DE IMPLANTES CON DIFERENTES DISEÑOS: UN ESTUDIO HISTOLÓGICO, IMMUNOHISTOQUÍMICO, MOLECULAR, DE RAYOS X DE ALTA RESOLUCIÓN EN ANIMAL

Tesis Doctoral

ENRICA GIAMMARINARO

Sevilla, 2024

Sevilla, Enero de 2024

EUGENIO VELASCO ORTEGA, Catedrático de Odontología Integrada de Adultos y Gerodontología de la Facultad de Odontología y Director del Máster de Implantología Oral de la Universidad de Sevilla.

SIMONE MARCONCINI, Doctor en Odontología y Director del Máster de Implantología Oral de Istituto Stomatologico Toscano.

CERTIFICAN:

Que Dª. ENRICA GIAMMARINARO, Graduada en Odontología por la Universidad de Pisa e inscrita en el programa de Doctorado de Ciencias de la Salud de la Universidad de Sevilla, ha realizado bajo su tutela y dirección el trabajo de investigación titulado **Colocación inmediata de implantes con diferentes diseños: un estudio histológico, immunohistoquímico, molecular, de rayos X de alta resolución en animal** que consideramos satisfactorio para optar al título de Doctor en Odontología.

Prof. Velasco Ortega Prof. Marconcini

DEDICATORIA

A mis padres Vito Giammarinaro y Francesca Barbera

A mi hermano, Pietro Ivan Giammarinaro

A mis Mentores

A futuros lectores

Intus et in cute

AGRADECIMIENTOS

Al Profesor EUGENIO VELASCO ORTEGA de la Facultad de Odontología de la Universidad de Sevilla, por servir de estímulo continuo y de ayuda concreta y por compartir sus conocimientos y sus recursos, que me han servido durante todo mi trabajo.

Al Doctor SIMONE MARCONCINI del Istituto Stomatologico Toscano, por su presencia continua, tangible e insustituible; por su libre confianza en mí y por hacerme creer que este camino era posible. Gracias por ser siempre tan Bueno y fuerte conmigo. No terminó aquí.

Al Profesor UGO COVANI del Istituto Stomatologico Toscano, por su ayuda concreta a lo largo de mis estudios y por servir de estímulo continuo de mi interés por la investigación y por compartir sus conocimientos y sus recursos; por abrirme la puerta de su casa cada vez que lo necesitaba.

A la Profesora ANNAMARIA GENOVESI del Istituto Stomatologico Toscano, por abrirme la puerta de su casa cada vez que lo necesitaba. Gracias por su ayuda real y por servir de estímulo continuo de mi interés por la investigación y por compartir sus recursos siempre.

Al Doctor ARIANO NAHI quien siempre me animó a ir más rápido.

A todos los profesores y compañeros de la Escuela de Especialización en cirugía oral de la Facultad de Odontología y de Odontología de Siena. Gracias por hacer que estos años sean tan reales.

A la Universidad de Sevilla, la institución que ha permitido mi formación investigadora en el Doctorado de Ciencias de la Salud que ha hecho posible la realización de mi trabajo de investigación para la tesis doctoral.

A mi familia sin espacio y sin tiempo.

TABLE OF CONTENTS

INTRODUCTION 1

1.Background 2

2. The periimplant mucosal attachment: definition and composition 9

3. The periimplant mucosal attachment may vary with the IAP 13

4. The periimplant mucosal attachment at immediate implants 16

5. Clinical relevance of the periimplant mucosal attachment 18

HYPOTHESIS 21

MATERIALS AND METHODS 23

1.Implant characteristics 24

2. Ethical statement 25

3. Experimental animals and housing 25

4. Experimental design 26

5. Surgical and terminal procedures 26

6. Samples preparation 28

7. Electron microscopy (EM) 29

7.1. Preparation and analysis of samples for EM 29

7.2. EM ultrastructural analysis of collagen bundles 29

7.3. EM Quantitative Analysis of Collagen Bundles 30

8. Statistical Analysis 31

RESULTS 32

1. Radiographic analysis 33

2. Histological Analysis 33

3. EM ultra-structual analysis of collagen fibers
in peri-implant soft tissue 34
4. EM quantitative analysis of collagen fiber bundles 36
5. Additional ultra-structural observations 39

DISCUSSION 42
1. Summary and Interpretation of Results 43
2. Ties back to the existing literature 45
3. Answers to the knowledge gap 47

CONCLUSIONS 53

REFERENCES 55

CURRICULUM VITAE AND RELATED PUBLICATIONS 66

INTRODUCTION

1. BACKGROUND

The use of dental implants for the rehabilitation of patients with single or multiple edentulism has become a common protocol, including, diagnosis, surgery, prosthetic, and maintenance, in daily dental practice, associated with high survival and success rates (Figure 1) [1-2].

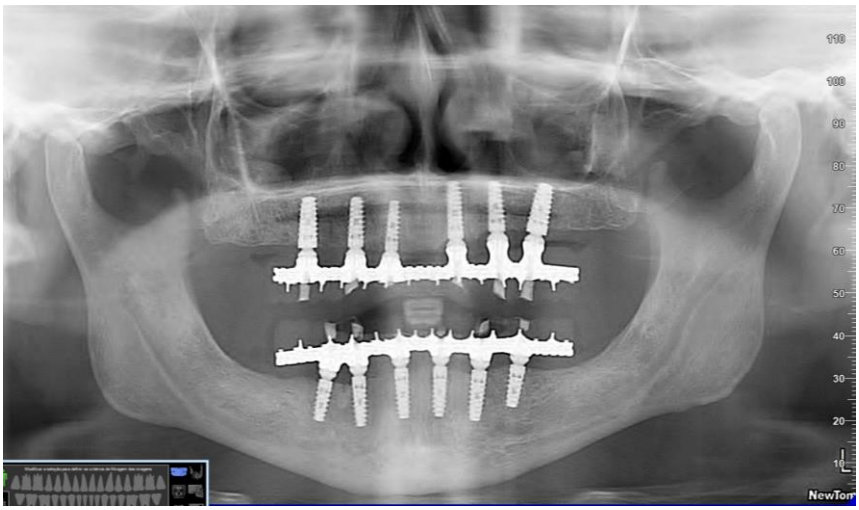

Figure 1
Panoramic imaging of edentulous patient treated with fixed rehabilitation with implants

Rehabilitation of edentulous patients can be obtained through different treatment options, such as complete dentures, removable implant-retained dentures, or fixed implant-supported dentures (Figure 1). When evaluating patient-centered treatment outcomes, fixed prostheses on osseointegrated implants provide the greatest satisfaction compared to removable ones. Based on this assumption, oral rehabilitation of edentulous patients with dental implants to support a provisional or definitive,

prosthesis by immediate loading is a growing and successful clinical option [1-2].

Furthermore, compared to conventional dental implant rehabilitation, this approach minimizes management costs, surgical need for bone augmentation, treatment intervals, treatment failure rate, and patient morbidity. Maintaining high quality of life and patient-perceived outcomes further support the treatment concept mentioned above [1-2].

The long-term success of dental implants depends on many factors, among those: the accurate diagnosis and treatment planning with regards to the patient's local and systemic risk factors, ideal implant position, implant type, implant-abutment connection type, prosthetic rehabilitation, and professional and domestic hygiene maintenance [3-4].

Overall the survival and success rates were satisfactory in many studies among patients treated with dental implants. However, a rate of the failures had occurred before the loading with abutment connection (early failures), which might have been due to the failure of bone healing around the implant and subsequent failure of osseointegration [4].

The introduction of osseointegrated implants in dentistry has revolutionized rehabilitation techniques for partially or totally edentulous patients. Initially, treatment with osseointegrated implants was developed, fundamentally, for the functional rehabilitation of patients with total edentulism. Since then, the rehabilitation of the edentulous patient with

dental implants has been a significant challenge for the professional due to the functional and aesthetic demands of the patients [3-4].

Figure 2
Clinical image of edentulous patient treated with maxillary fixed rehabilitation with implants

Fixed rehabilitation on implants in edentulous patients proved to be an important treatment alternative, accompanied by a high success rate in edentulous patients. This treatment has been scientifically documented and validated over the last four decades. The possibility of performing surgical and prosthetic techniques in a short operating session represents a good implantology alternative since it significantly reduces treatment time and improves the quality of life of patients in a very positive way [3-4].

It is well known that osseointegration without the long-term stability of hard and soft tissues is not sufficient *per se*. In particular, poor quantity

and quality of peri-implant soft tissues are associated with clinical failure of the implant [5].

The stability of peri-implant tissues can be influenced by various etiological factors such as factors related to the patient (systemic diseases, smoking, periodontal background, oral hygiene, parafunctional habits), with implant surgery (bone volume and quality, presence of keratinized gingiva, surgical technique as submerged or non-submerged technique), with the characteristics of the implant (type of surface, macrodesign, type of connection) and with the prosthetic design (retention, type of abutments, prosthetic structure)(Figure 3) [5].

Figure 3
Clinical image of insertion of an implant in anterior maxilla

The stability of hard and soft tissues around dental implants has been recognized to be a key factor for long-term implant success. Clasically, a

vertical crestal bone loss of 1 to 1.5 mm during the first year of function followed by a marginal bone loss of 0.2 mm per year has been reported in several studies. However, during last years the experimental and clinical research reported a minor marginal crestal bone accepted as success when specific biological and implant factors are considered (Figure 4) [4-5].

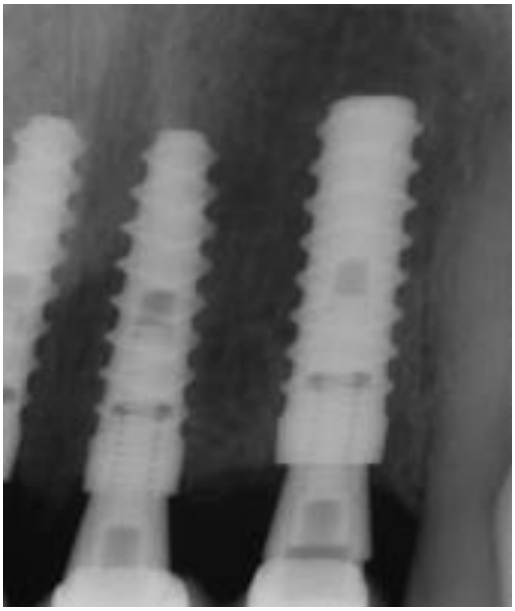

Figure 4
Radiographic control of crestal bone in patient treated with maxillary implants

The integrity of both the epithelial lining and the supracrestal connective tissue is required to maintain implant health for a long time [6-7]. Recently, few authors have contributed to the redefinition of peri-implant mucosa, providing the term "implant supracrestal complex" (ISC) [8]. The ISC includes the peri-implant tissue - the sulcus, the junctional epithelium, the connective tissue - and the implant-abutment-prosthesis (IAP) complex. Thus, it is unreasonable to speak of supracrestal tissues without mentioning the type and location of the implant/abutment interface (Figure 5).

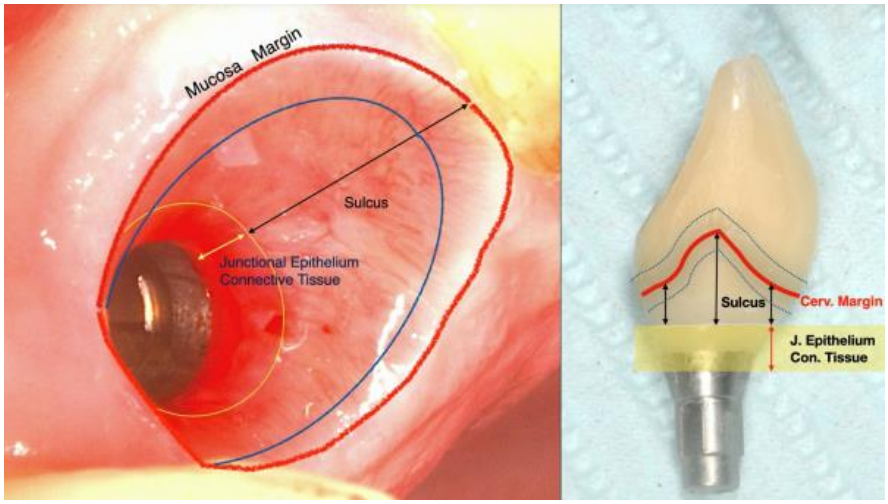

Figure 5
Implant Supracrestal Complex" (ISC) [8]
Peri-implant tissue - the sulcus, the junctional epithelium, the connective tissue - and the implant-abutment-prosthesis complex

Today, there is an increasing scientifc evidence about the interrelations between the condition of the peri-implant tissue and the implant-abutment-prosthesis complex, in a contaminated enviroment with the presence of oral bacteria. In fact, several factors as the configuration of implant-abutment complex and prosthesis design and retention can influence on clinical outcomes of treatment with dental implants [8].

This implant supracrestal complex perfomed an anatomic and functional interaction of the mechanical components and the biologic tissues, that is a well concept of health, however, this comprehensive system can manifest clinical problems (biological and technical complications) [8].

Also, the establishment of the supracrestal attachment may vary in the case of immediate implants. In 2004, the third ITI Consensus Conference proposed a classification system for the timing of implant placement. There was consensus that such a classification based on morphologic, dimensional, and histologic changes that follow tooth extraction and on common practice derived from clinical experience. [9].

Type I refers to implant placement immediately following tooth extraction and as part of the same surgical procedure; Type II refers to placement of the implant when complete soft tissue coverage of the socket is achieved (typically 4 to 8 weeks); Type III refers to implant placement when there is evidence of substantial clinical and/or radiographic bone fill of the socket (typically 12 to 16 weeks); Type IV refers to implant placement in a completely healed site (typically more than16 weeks) [9].

There is extensive evidence that immediate implants display survival and success rates comparable to delayed ones but with the clear benefit of a faster treatment schedule [10]. Of course, there are disadvantages as well, namely: the site morphology may complicate optimal placement and anchorage; thin tissue biotype may compromise the outcome; there could be a lack of keratinized mucosa for flap adaptation; adjunctive surgical procedures may be required; the procedure is highly technique-sensitive.

The supracrestal tissue formation at immediate implants may be managed with different surgical and prosthetic strategies, eventually

leading to the preservation or amelioration of the hard and soft tissue volume and quality at the crestal level [11]. There is evidence that the use of bone grafting materials, connective tissue grafts, healing screws, and immediate provisionalization can prevent soft tissue shrinkage at immediate implants (Figure 6) [12-17].

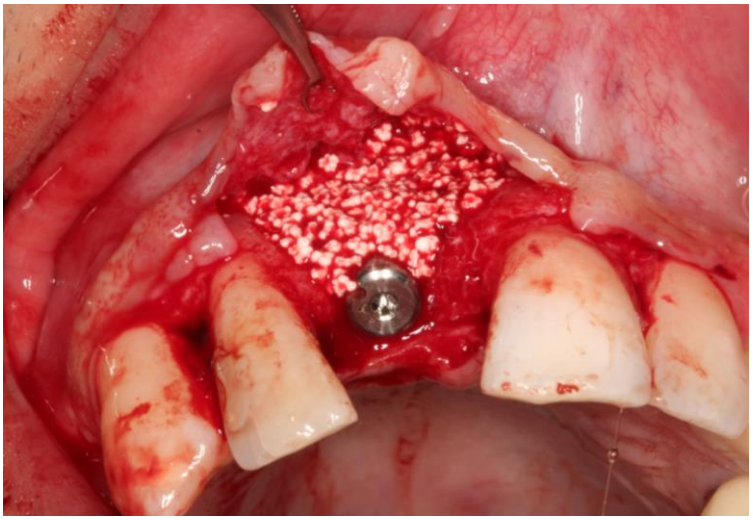

Figure 6
Clinical image of use of bone graft material

2. THE PERIIMPLANT MUCOSAL ATTACHMENT: DEFINITION AND COMPOSITION

Peri-implant mucosal attachment plays a key, pivotal role as a barrier interposed between the oral cavity and the mineralized tissues around the implant, to obtain long-term aesthetic and functional implant success and survival [18]. After implant insertion, the early healing period of formation and maturation of this mucosal attachment, is comprised between 6 to 12

weeks[18].

From apical to coronal in the vertical direction, the tissues of the ISC are defined by the marginal bone (MB), the connective tissue (CT), the junctional epithelium (JE), and the sulcus, along with the sulcular epithelium [8]. The CT and the JE, taken together, on average, occupy between 3 and 4.5 mm in a vertical dimension (Figure 7)[19-20].

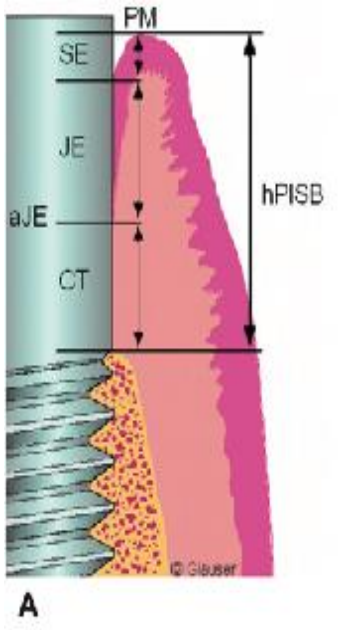

Figure 7
Schematic representation of the peri-implant mucosal attachment [21]

In a histologic study performed on mini-implants retrieved from humans, Glauser et al [21] described the supracrestal attachment in detail (Figures 7-8) [21]. The cells of the JE established the epithelial attachment to the implant surface. The width of the JE ranged between 1.8 mm and 3.4

mm. The implant surface between the most apical cells of the JE and the alveolar crest was in all ground sections in direct contact with the supracrestal connective tissue. In an approximately 100 to 150 µm–wide area adjacent to the implant surface, the connective tissue was, in general, free from blood vessels and was dominated by collagen fibers oriented parallel to the longitudinal axis of the implant.

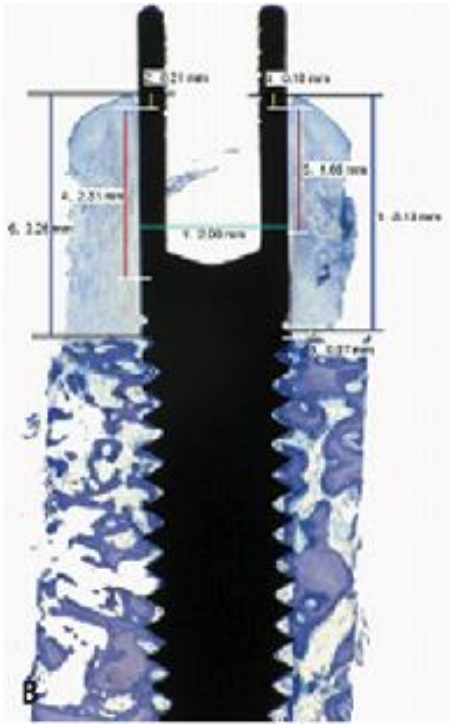

Figure 8.
Histologic exam of the peri-implant mucosal attachment [21]

Adjacent to this area, the connective tissue was densely packed with collagen fibers oriented circumferentially around the implants. The average height of CT ranged between 2.1 and 0.6 mm. Overall, the height of the

periimplant soft tissue barrier, consistent an epithelial and a supracrestal connective tissue revealed a mean value of 4.0 mm-4.5 mm, depending on the implant surface.

In two human autopsy specimens the height of the connective tissue component was found to be, respectively, 1.9 +/- 0.2 mm in the mandible, and 2.5 +/- 1.3 mm in the maxilla and 1.6 +/0.4 in the mandible [22-23]. The first study report the histological features found around three non-submerged titanium plasma-sprayed implants retrieved, after a 10-month loading period, from an autopsy case [22]. The implants were surrounded by connective tissue. No inflammatory infiltrate was present in the epithelium and in the supracrestal connective tissues. The fibers of this tissue had a different orientation: in the most coronal portion of the implants (smooth surface), they tended to run parallel implant's surface, while in the most apical region (plasma-sprayed surface), they tended to be arranged in a perpendicular fashion [22].

The second study, report the importance of the soft tissue reaction and biologic width in the success of oral implants [23]. Several implants were placed in the maxilla and mandible of a smoking patient and were loaded immediately with fixed temporary restorations. The biologic width, sulcular epithelium, and connective tissue were longer than in the mandible, except the junctional epithelium [23].

3. THE PERIIMPLANT MUCOSAL ATTACHMENT MAY VARY WITH THE IAP

Classical histologic studies have described the arrangement of connective tissue fibers around the implant in dogs and humans, documenting the presence of parallel to long-axis, circular or ring- shaped, or inserted fibers [24-26].

An experimental study assesses the marginal periimplant tissues at intentionally non-submerged and initially submerged and subsequently exposed implants in 5 beagle dogs [25]. Three implants systems were used. The mucosal barrier which formed to the titanium surface following implant installations comprised an epithelial and a connective tissue component, with similar dimensions and composition. The study suggested that correctly performed implant insertion may ensure soft tissue healing, and that the macroscopic and surface design of the titanium implant seems a limited importance [25].

The scientific evidence demonstrates that the formation of the biological width and maturation of the barrier function around transmucosal implants requires aproximately 6–8 weeks of healing [26]. The established peri-implant soft connective tissue resembles a healing tissue in composition, fibre orientation, and vasculature. The peri-implant junctional epithelium may vary a greater final length under certain biological and clinical conditions such as the presence of keratinized mucosa and implants

inserted in fresh extraction sockets compared with conventional implant procedures in healed sites [26].

However, collagen fibers are not predetermined, yet they depend on the local environment. For instance, Rodriguez-Ciurana and cols [27] reported that around implants with a platform switching design, circular orientation of collagen fiber was observed as the main arrangement in a cross-sectional view. They argued that by increasing the room for soft tissue by changing the design of the abutment or its transversal discrepancy with respect to the implant platform, the supra- crestal connective tissue fibers would be retained in a stable coronal position [27].

Abutment structure and design has been suggested to have a relevant role in the formation of the peri-implant soft tissues, their aesthetics and their long-term stability [28]. Over the past years, many different abutment shapes have been proposed in the literature, from scalloped and platform-switched designs to concave abutments; these latter abutments present an inward narrowed profile that produces a macroscopic groove.

The abutment design and structure can influence in the histologic analysis of peri-implant connective tissue. In fact, recent evidence suggested that divergent or convergent macro-geometry and different treated surfaces reported differences in connective tissue vertical dimension and greater amount of collagen bundles that improving a peri-implant soft health [28].

The hypothesis is that this particular macrostructure of the abutment could led to a much better stability of the peri-implant soft tissues. This concave aspect could produce an empty space, providing a conducive environment for the formation of a blood clot, migration and proliferation of connective tissue cells, extracellular matrix protein deposition and adsorption, granulation tissue formation, matrix remodeling, an increased length of contact between soft tissues and abutments and a higher connective tissue adhesion and thickness, with an increased tissue stability with higher mechanical properties [18,29-30].

Rompen et al. [29] reported that a concave transmucosal design determined, in the aesthetic area, an improved stability of the soft tissues, in comparison to divergent transmucosal abutments. Moreover, experimental and clinical evidence have shown similar an stability of soft tissue integration at one-piece implants and at abutments of two-piece implant systems [29].

Chien et al. [30] spoke of a collagen tissue formation driven by a groove. These authors found, in an animal experimental study, that the JE level showed dense circular fibers surrounding the abutment, with an organization of the circular gingival fibers and the associated fibroblastic cells. The histologic analysis have shown that collagen fibers in concave abutments were more dense and well organized, with a significantly lesser peri-implant bone resorption. Under higher magnification, it was possible

to observe that the collagen fiber bundles were perpendicularly or obliquely oriented toward the concave abutment surface [30].

Also Hu et al. [31] found, in another animal study, that the use of concave abutments produced lesser bone resorption and a higher connective tissues attachment when compared with straight abutments. Radiographic and histometric analysis showed that least bone resorption occurred around concave abutment implants and greatest bone resorption around conventional abutment implants. Histometric findings showed that highest connective tissue attachment and shortest biological width had formed around concave abutment implants [31].

On the contrary, Delgado-Ruiz et al. [32] reported, in another animal study, that a concave abutment determined a lower thickness of the peri-implant soft tissues. The study describes histologic characteristics of connective tissue fibers around healing abutments of different geometries (concave and wider healing). The total thickness of connective tissue in the horizontal direction was greater in wider healing abutments. The orientation of the fibers showed a higher percentage of parallel fibers in concave abutments and a higher percentage of oblique fibers in wider abutments [32].

4. THE PERIIMPLANT MUCOSAL ATTACHMENT AT IMMEDIATE IMPLANTS

Immediate post-extractive implants are often associated with a

reduced amount of available peri-implant hard and soft tissue; both of which require correction through osseous reconstructive or regenerative and/or oral plastic surgical techniques [33].

The immediate implant placement after tooth extraction may constitute an important challenge for the oral surgeon. The reduced alveolar bone, size and shape, presents several problems for the insertion of implant with a primary stability. Frequently, it is necesary the use of grafting material, as autogenous bone, demineralised bovine bone, demineralised freeze-dried bone allograft and synthetic bone materials. The use of these grafting materials (and membranes) were to fill the gaps between implants and socket walls for the treatment of bone defects and fenestrations [33].

The experimental and clinical research have demonstrated several morphological modifications of the height and width of the alveolar ridge following tooth extractions [34]. The healing process following tooth extraction frequently resulted in more pronounced resorption on the buccal than on the lingual/palatal aspects of the alveolar ridge. This histological process that resulted in hard and soft tissues reduction seemed to be more pronounced during the initial phase of wound healing than during later periods after tooth extraction. In the healing process of a post-extractive socket, bone resorption proceeds in all directions, and such a remodeling may cause an alteration of the soft tissue contour [34].

It has also been shown that the mechanical status of the bone–

implant interface is an important determinant for both osseointegration and long-term implant success [35]. The implant-abutment connection can present different designs depending on its geometric features. Some types of design increases the implant-abutment contact area and improves the distribution of forces, providing better stability, and bacterial seal. Also, the presence of design features of connections prevents several movements as rotation between the components of the system. This functional integrity is very important for long-term stability of peri-implant hard and soft tissues [35].

In the case of immediate implants, the local environment is absolutely peculiar: there is always a discrepancy between the implant bed preparation and the tissues interface, thus the surface of the abutment, the implant–abutment interface, the type of implant connection, and the collar design can all influence the remodeling process of peri-implant and consequently the maintenance of crestal bone and soft tissue levels [15-17,33].

5. CLINICAL RELEVANCE OF THE PERIIMPLANT MUCOSAL ATTACHMENT.

The treatment of partially and totally edentulous patients with dental implants is considered a predictable therapeutic option for the prosthetic rehabilitation of oral function and loss aesthetic with long-term clinical outcomes. Tissue deficiencies at implant locations are frequent clinical problems, that may increase the marginal bone loss, mucosal inflammation, and soft-tissue recession [36].

Taking into consideration the above information, it becomes important to establish a minimum peri- implant supracrestal vertical tissue height of about 3 to 4.5 mm that will adequately accommodate the biologic demands of sustainable health. In cases where the vertical height of the peri-implant tissue is less than 3 mm, marginal bone resorption has often been reported around the implant platform [36].

This might be a physiologic remodeling that results in reestablishing the vertical dimensions required to accommodate the soft tissues at the expense of the crestal peri-implant bone. Several researchers have correlated this pattern of early bone resorption and preoperative supracrestal gingival tissue height [37-38].

The scientific evidence reports the influence of soft tissue grafting procedures on peri-implant health. The clinical outcomes revealed that soft tissue grafting using autogenous tissue can improve the amount of keratinized tissue with better results of mucosal status that are very important for the long-term maintenance of implant treatment. In fact, soft tissue grafting increases the mucosal thickness and reduces the marginal bone loss [37].

The clinical experience have demonstrated the critical role of peri-implant soft tissue on implant esthetics and health in long-term success of the treatment with dental implants. Several studies have reported the negative influence of an insufficient amount of keratinized mucosa width

around dental implants, can be related with more plaque accumulation, mucosal inflammation and recession and following attachment loss [38].

The comprehensive clinical approach of the oral surgeon have reported the importance of the diagnosis, planning, and treatment of soft tissues in the maintenance of peri-implant status. Several patient factors including the control of systemic disease, assessment of hard and soft tissues status, the incorporation of a permanent oral hygiene improves peri-implant health. Clinician factors such as the implant position, excess cement, and restorative design can contribute to development of peri-implant disease. Survillance of implant status is essential and can be assisted by the evaluation of risk factors, establishment of a proper recall program, and monitoring changes in bone and peri-implant tissues [38].

HYPOTHESIS

HYPOTHESIS

Documenting the topography and morphological properties of collagen fibers around the implant neck is essential if we are to understand how alterations in the direction, periodicity, and/or diameter of collagen fibers, can affect the bio-mechanical behavior of the peri-implant mucosa.

Collagen self-assembly is an entropy-driven process caused by the loss of water between monomers, and the self-assembly process is mainly divided into two stages: nucleation and growth. Within limits, that entropy could be conveyed in the desired direction during wound healing/in the case of immediate implant positioning.

The geometry of extracellular matrices or the implant macro-geometry by using mechanical/geometrical cues might modulate connective tissue behavior. In the present doctoral animal study, it was hypothesized that a concave implant neck might trigger spontaneous alignment of the collagenous network, thus affecting fibroblast polarization, migration, and fibers growth direction and arrangement as well.

Two implants with identical bodies but different healing abutment geometries were compared: the Test one presented a 2 mm concave area above the implant platform, chosen according to the positive results reported in a histological animal study and a clinical study with a similar concave profile, whereas the Control abutment had a parallel-walled healing screw.

MATERIALS AND METHODS

1. IMPLANT CHARACTERISTICS

All implants were tapered shaped (IK Internal Hexagon, RESISTA® Company, Ing. Carlo Alberto Issoglio & C. S.r.l., Omegna, Italy). Test abutments (TEST) presented a 2 mm height concave portion with a double acid-etched (DAE) surface, whereas Control ones (CTRL) were parallel-walled shaped with a DAE surface. Both presented a 4 mm diameter switching platform and a length of 10 mm (Figure 1).

Figure 1. (a) Test implant and abutment(TEST); (b) Optical microscopy images of TEST implant (on the left) and Control implant (CTRL, on the right).

2. ETHICAL STATEMENT

This animal study was performed in the Servicio de Animales de Experimentación (SAEX) at the Faculty of Veterinary of the University of Córdoba.

The experimental study was approved by the Animal Ethical Committee of the Junta de Andalucia, Consejeria de Agricultura, Ganaderia, Pesca y Desarollo Sostenible on December 14, 2021 (n° 29/11/2021/184). All procedures were performed in accordance with Spain's animal protection law and according to the Animal Research: Reporting of in Vivo Experiments (ARRIVE) [39] guidelines in a randomized prospective design.

3. EXPERIMENTAL ANIMALS AND HOUSING

Two swine (sus scrofa), aged on average three years old, were acclimated for a three-week period prior to the initiation of the study. The two animals were identified using an ear tag. An antibiotic- free diet, softened by soaking in water, was provided. Water was available ad-libitum. The person in charge of the animals' welfare took care of aeration and food and water administration, as well as the animals' behavioral and health conditions throughout the study period. The whole study was accompanied and monitored by a veterinarian, and surgeons with extensive experience performed all surgical procedures.

4. EXPERIMENTAL DESIGN

Animals had implants placed in the left or right mandibular alveolar ridges. Implants were either placed in the physiological mature bone present between the lower canine and first premolar or at the mandibular premolar region, within tooth extraction sites. All implants received a healing abutment at the time of placement. Implants were allowed three weeks of healing.

Each animal received 6 implants, 3 per hemimandible. CTRL and TEST implants were positioned across the jaw in a symmetrical and well-controlled manner. A total of 12 weeks after the implant placement, all animals were euthanized. Therefore, a total of 12 implants were placed. 2 CTRL implants and 2 TEST implants were excluded from further analysis because of early implant failure. In the end, a total of 8 implants were analyzed (CTRL, n = 4 and TEST, n = 4).

5. SURGICAL AND TERMINAL PROCEDURES

Before surgical intervention, animals were fasted overnight and weighed. On the day of surgery, all animals were anesthetized with intramuscular (IM) medetomidina 0.05 mg/kg + Zoletil (zolacepam + tiletamina) 3 mg/kg.

After that, a mask inhalation of 2–5% of Isoflurane mixed with oxygen was administered. Animals were transferred to the surgical area and

intubated with an endotracheal tube, after which general anesthesia continued with 2–5% of Isoflurane. Monitoring of heart rate, blood oxygen saturation, and blood pressure occurred during the entirety of the procedures, as well as the post-operative period.

All surgical procedures were performed under aseptic conditions in an animal operating theater under general anesthesia. Tooth extraction was carefully completed: for all teeth, gentle pressure was applied to the gingival sulcus using a small periosteal elevator, after which mandibular premolars and molars were sectioned in a buccolingual direction at the furcation between the mesial and distal root. A rotary instrument was used for sectioning; then, a straight elevator was used to confirm sectioning. After that, the mesial and distal roots were elevated and removed using dental forceps.

In mature sites, a No. 15c blade was used to create a midcrestal incision in the area between the canine and the first premolar. A full-thickness mucoperiosteal flap was elevated and implants were placed at least 1.5 mm apart from the neighboring teeth and housed within the buccal and lingual plates using manufacturer guidelines for drilling protocol. Healing abutments were placed, and the site was closed with 4–0 silk sutures. All implants were placed equicrestally, and no bone graft was placed.

Within the first days after surgery, all animals were monitored routinely, and further analgesia was given if necessary. Post-operative surgical pain was relieved using 0.12–0.24 mg/kg buprenorphine HCl, administered subcutaneously (SC). Animals were sacrificed 12 weeks after

surgery. Following sedation using the aforementioned agents, cardiac arrest was induced by administration of 110 mg/ kg Pentobarbital intravenously (IV) at each previously mentioned timepoint.

6. SAMPLES PREPARATION

Block sections were retrieved using an oscillating autopsy saw to keep the soft tissue intact. Samples of peri-implant soft tissues for histological analysis were fixed by immersion in 10% buffered formalin, dehydrated in increasing series of alcoholic rinses, and finally embedded in glycol-methacrylate resin (Technovit 7200 VLC, Wehrheim, Germany).

The specimens were processed according to the protocol described in a previous study by Iezzi et al [40]. Briefly, they were sectioned along its longitudinal axis to obtain histological longitudinal sections of the peri-implant tissues. Histological analysis was carried out under a light microscope (Laborlux S, Wetzlar, Germany) connected to a high-resolution video camera (3CCD, JVCKY-F55B, JVC, Yokohama, Japan) and interfaced with a PC.

Samples of peri-implant soft tissues for transmission electron microscopy (TEM) analysis, instead, were preserved in 3.5% glutaraldehyde in 0.1 M sodium cacodylate (NaCaCO) buffer.

7. ELECTRON MICROSCOPY (EM)

7.1.PREPARATION AND ANALYSIS OF SAMPLES FOR EM

All implants and associated adjacent peri-implant soft tissues were removed from the mandible of each swine. 4 specimens were retrieved around parallel-walled abutments (CTRL) and 4 specimens around concave abutments (TEST) and fixed at room temperature (RT) with 3.5% glutaraldehyde in 0.1 M NaCaCO buffer (pH 7.2) and stored at 4 ◦C in the fixative until shipment. Small portions of fixed soft tissues carefully dissected from the area around the implant were rinsed in 0.1 M NaCaCO buffer and then, post-fixed 2% osmium tetroxide (OsO4) in the same buffer for 1 h, block- stained with saturated uranyl acetate, rapidly dehydrated in graded ethanol and acetone, and embedded in epoxy resin (Epon 812)[41].

For electron microscopy (EM), ultrathin sections (~40 nm) were cut in a Leica Ultracut R microtome (Leica Microsystem, Wetzlar, Germany), using a Diatome diamond knife (Diatome Ltd., Biel, Switzerland), and after double staining with uranyl acetate and lead citrate, they were examined at 60 kV with an FP 505 Morgagni Series 268D electron microscope (FEI Company, Brno, Czech Republic), equipped with a Megaview III digital camera (Olympus, Tokyo, Japan) and Soft Imaging System (GmbH, Munster, Germany).

7.2.EM ULTRASTRUCTURAL ANALYSIS OF COLLAGEN BUNDLES

For EM qualitative and quantitative analysis small samples were taken from a ring of tissue dissected all around the area of the abutment.

The ultrastructural analysis of collagen from peri- implant soft tissues was mostly performed in images showing the cross-sectional appearance of the collagen fibers, taken from longitudinal sections of the tissues. Only sample regions near the abutment surface (CTRL, n = 4 and TEST, n = 4) were observed.

7.3.EM QUANTITATIVE ANALYSIS OF COLLAGEN BUNDLES

For quantitative analysis, 15 micrographs/group were randomly collected from non-overlapping regions at 7100× of magnification and used for the following quantitative analysis:

(i) In each micrograph, the total area covered by collagen bundles was evaluated by drawing the outline of each bundle using the Soft Imaging System (GmbH, Muenster, Germany). All measured bundle values were then mathematically summarized. Only cross-sectioned bundles with a minimum size of 0.5 μm2, where collagen fibers were distinguishable and not longitudinally oriented, were considered for the analysis. Considering that each micrograph at 7100× of magnification covers 142.6 μm2 of sample, the relative presence of collagen bundles (%) in each sample was obtained by dividing the number of total outlined collagen fibers (in μm2) by the total area of analyzed samples (i.e., 142.6 μm2 × 15 micrographs).

(ii) In each micrograph, the number of longitudinally oriented bundles of collagen (of different sizes) was counted and reported as mean ± standard error of the mean (SEM) in 100 μm2.

8. STATISTICAL ANALYSIS

In all comparisons performed between CTRL and TEST conditions, not normally distributed data were found and analyzed using a non-parametric t-test (Mann–Whitney test). The experimental values were elaborated using the statistical software package GraphPad Prism Software Analysis version 9.0 (San Diego, CA, USA), and the statistical significance of the differences between the groups was determined for a $p < 0.05$. Data were expressed as the mean ± SEM or standard deviation (SD).

RESULTS

1. RADIOGRAPHIC ANALYSIS

After 12 weeks, proper histologic healing was observed around both CTRL and TEST implants. The radiographic exams also revealed a good osseointegration of all implants (Figure 1).

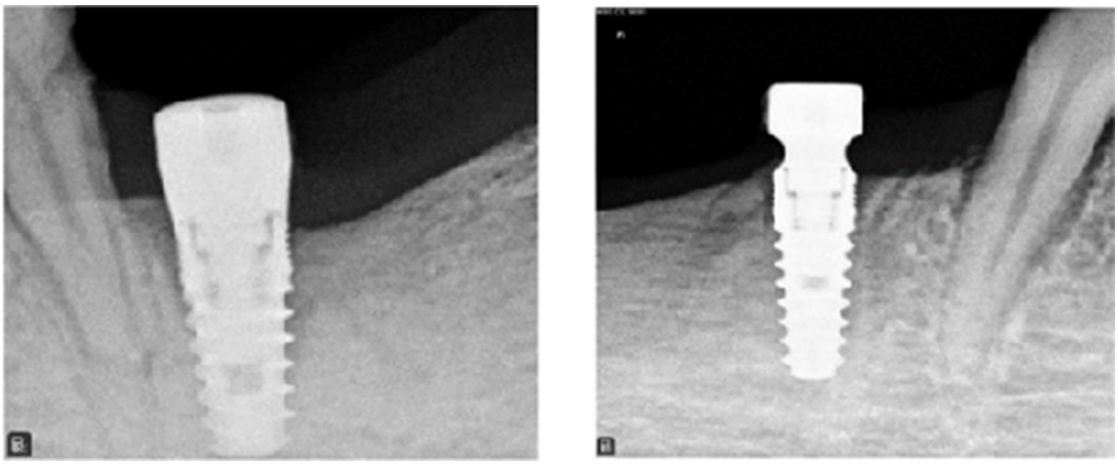

Figure 1. Representative intraoral radiographs presenting two implants placed in extractive sites of two premolars at the 3-month follow-up visit. A Control implant with a parallel-walled abutment on the left, and a Test implant with a concave profile abutment on the right.

2. HISTOLOGICAL ANALYSIS

For histological analysis, transversal undecalcified sections were obtained. Histological results (Figure 2) showed the presence of peri-implant soft tissues in close connection with both Test and Control abutments. However, although this is only a qualitative finding, the soft tissue appears more adherent to the concave abutment than the straight one.

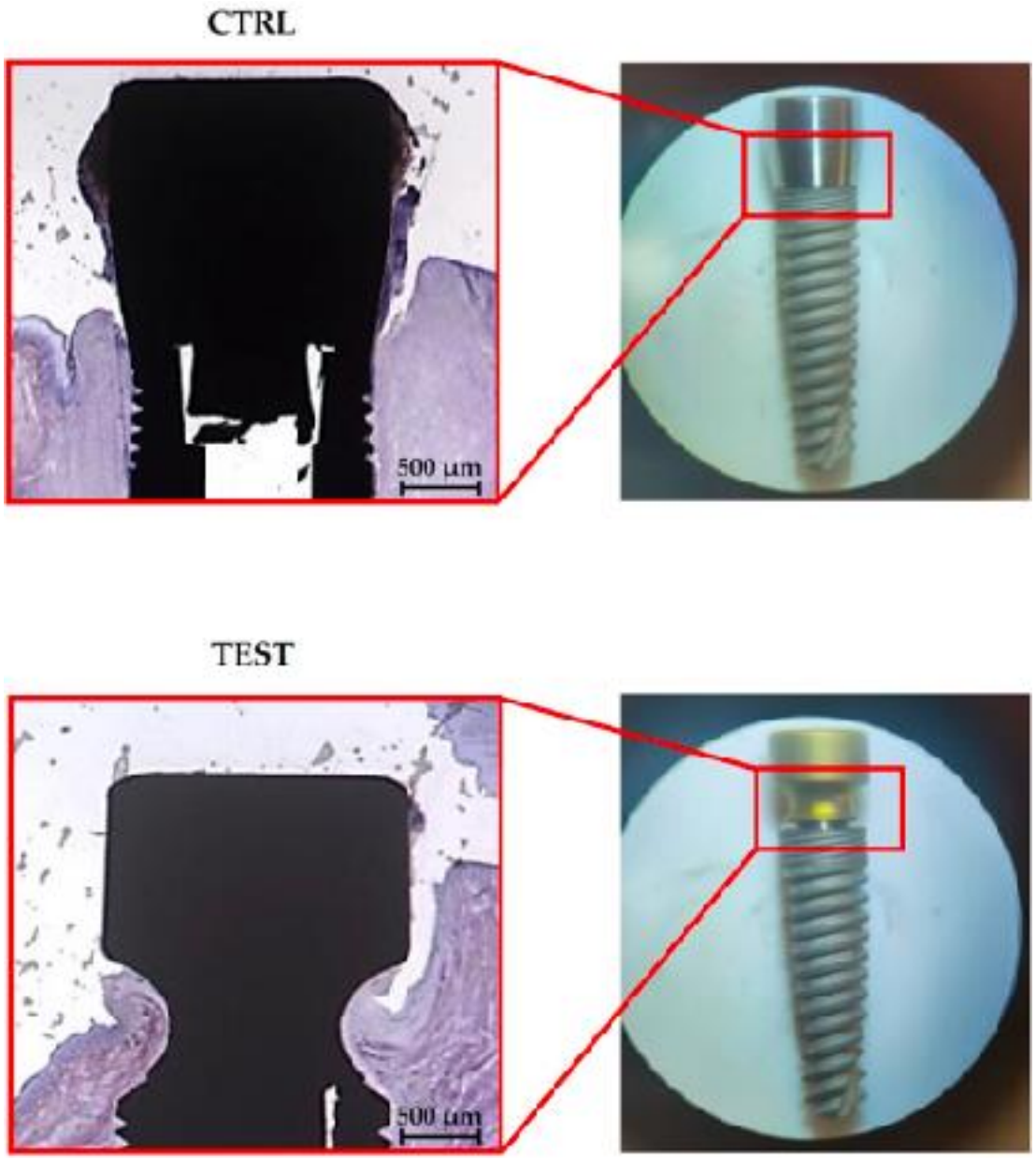

Figure 2. Histological longitudinal sections of the implant–abutment units. In the upper part, soft tissues surround the CTRL abutment. In the lower part, soft tissues surround the TEST abutment. (Acid fuchsin-Toluidine blue 20×).

3. EM ULTRA-STRUCTURAL ANALYSIS OF COLLAGEN FIBERS IN PERI-IMPLANT SOFT TISSUE

Ultrastructural analysis of the peri-implant soft tissue taken from sites in close proximity to the two different implants (Control and Test)

was initially performed blinded. At the EM analysis, peri- implant soft tissues were primarily constituted by collagen fiber bundles and cells.

Collagen fibers appeared as several long, parallel, and straight tubules, which were quite regularly arranged in bundles of heterogenous size (Figure 3A, “l”).

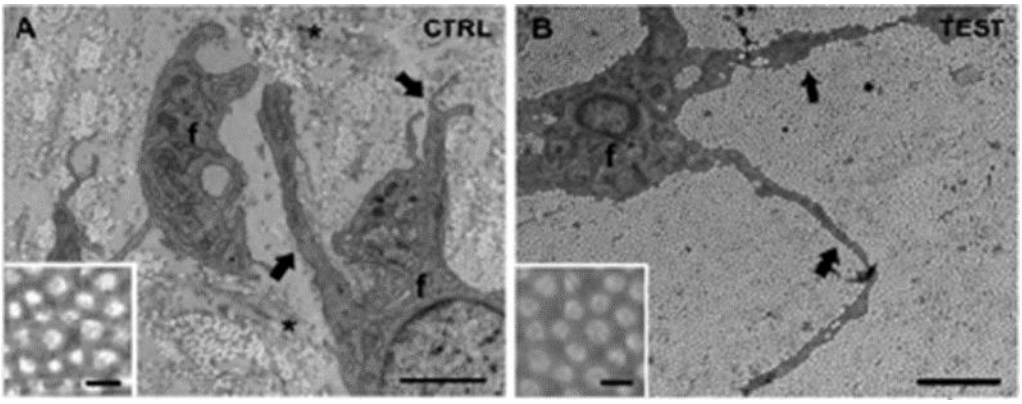

Figure 3. Representative electron microscopy (EM) images of peri-implant soft tissues. (A) The peri-implant soft tissue is primarily constituted by collagen fiber bundles (“c” and “l”) and fibroblasts (f); (B) in CTRL samples only few collagen fibers assembled, forming small, scattered bundles, compared to Test samples (TEST), where collagen bundles were thick, and often covered a large area of the analyzed section. Black arrows point to fibroblast processes. Scale bars: 2 µm; inset, 0.5 µm.

Cell populations of the peri-implant soft tissues were mostly constituted by fibroblasts (Figure 3, f), which exhibited a stellate appearance (note how fibroblast processes segregated individual collagen bundles, Figure 3, black arrows). Interestingly, during the EM analysis of the cross-sectioned collagen bundles at low magnification images (7.1k), the presence of different structural arrangements of collagen fibers between samples was quite evident.

Specifically, comparing the different appearance of collagen distribution and organization allowed us to divide samples into two groups:

Control specimens, in which an extensive aggregation of thick collagen bundles was rare or absent (Figure 3B), and Test samples containing a high-density large aggregation of tightly packed and sorted collagen fiber bundles (Figure 3C). Particularly, in Control samples (Figure 3B), the collagen matrix was composed of several small collagen bundles randomly distributed in the extracellular space at variable distances from each other.

On the contrary, large areas were observed in Test samples, where very thick collagen bundles were densely packed with each other without leaving sufficient space for the extracellular material (Figure 3C). These data, for the first time, suggest a different growth and assembly of the collagen matrix around Test abutments when compared to Control abutments. The concave shape seemed to determine an increased bundles' size of collagen fibers.

4. EM QUANTITATIVE ANALYSIS OF COLLAGEN FIBER BUNDLES

In order to confirm the obtained qualitative results, a quantitative EM analysis of images was performed. More in detail, from cross-sectional Control and Test images of the area of interest, the following were evaluated: (i) the percentage of the analyzed total surface area covered by collagen fibers (Figure 4E); (ii) the average size of collagen bundles (Figure 4F); (iii) the number of transversely oriented collagen bundles per 100 mm2 (Figure 4B and D).

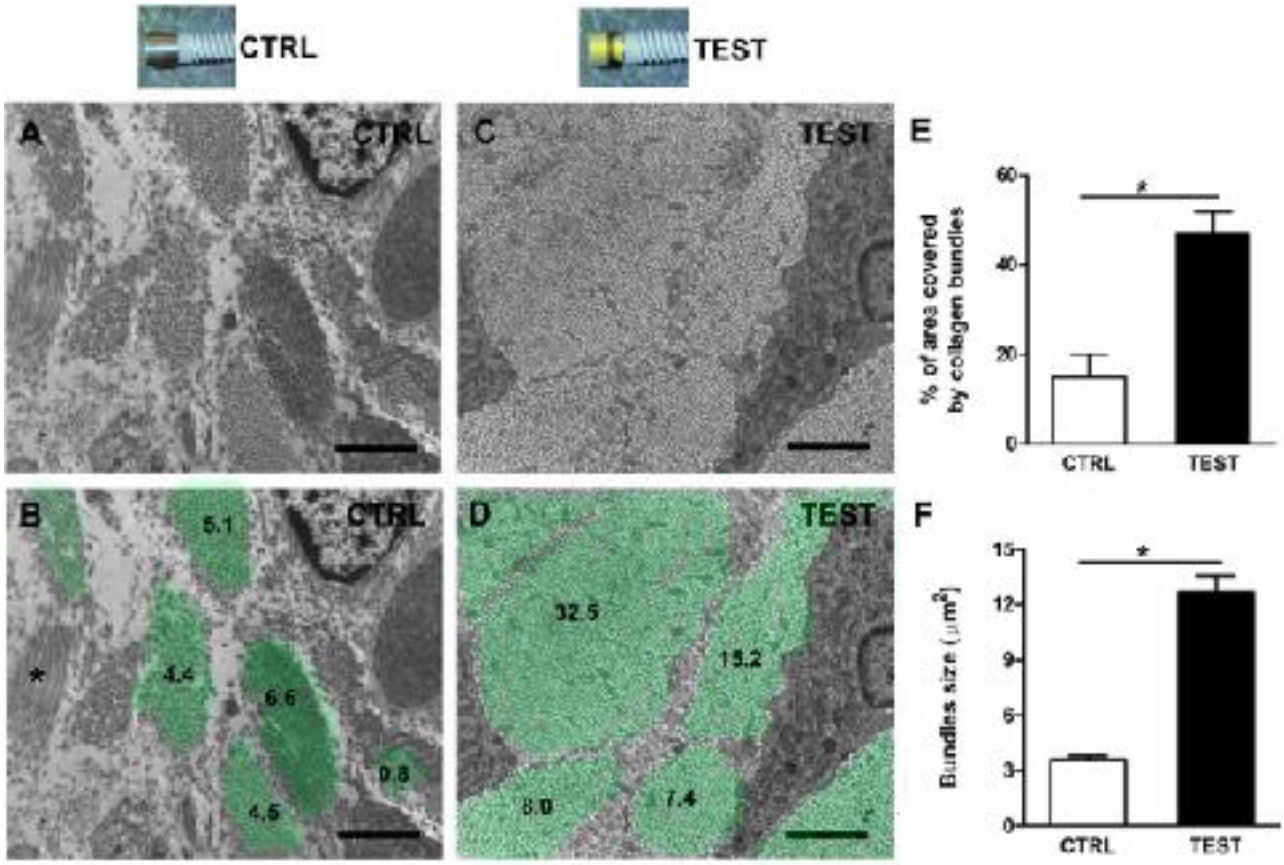

Figure 4. EM quantitative analysis of cross-sectioned collagen fiber bundles from CTRL and TEST samples. Representative EM longitudinal images of collagen fiber bundles around (A) CTRL and (C) TEST samples, (B,D) and corresponding collagen bundles' surfaces are highlighted in light green. Numbers refer to bundles' surface areas in μm2. Asterisk in panel (B) (*) refers to a longitudinal collagen fiber bundle; (E) Bar plot showing the quantitative analysis of the percentage of the analyzed area covered by collagen fibers; (F) Average size of the collagen bundles. Scale bars: 2 μm. * $p < 0.05$.

To better allow the visualization of collagen bundles' size, their surfaces have been highlighted with light green in the longitudinal images (Figure 4B,D). The mathematical The mathematical sum of each value gave a representative percentage of the surface area covered by collagen and the results have been reported numerically in Figures 4B and D.

RESULTS

Quantitative analysis of the total surface area covered by collagen fibers indicated that the use of Test implants was quite effective in aiding the formation and aggregation of collagen bundles in larger areas than Control ones. Notably, the percentage of total surface covered by collagen was approximately 47% in Test samples in respect to 18% of Control samples (Figure 4E and Table 1), resulting significantly higher.

	Sample 1	**Sample 2**	**Sample 3**	**Sample 4**
CTRL	18±5	28±3	8±3	5±1
TEST	47*±11	46*±6	63*±10	43*±19

Table 1. Percentages of the analyzed area covered by collagen bundles. Data are shown as mean ± standard error of the mean (SEM) (* p< 0.05 vs CTRL).

Furthermore, the use of Test abutments was also effective in significantly increasing the average size of a single collagen bundle, from 4 µm2 to 13 µm2 (Figure 4F and Table 2). The number of transversely oriented collagen bundles per 100 µm2 was lower in Test samples than in Control samples (Figures 4B and D).

	Sample 1	**Sample 2**	**Sample 3**	**Sample 4**
CTRL	4.2 ± 0.8	4.7 ± 0.4	2.6 ± 0.5	1.5 ± 0.2
TEST	20.7 ± 4.0*	7.5 ± 0.7	23.7 ± 2.8*	12.6 ± 1.9*

Table 2. Bundles size (µm2). Data are shown as mean ± SEM (* p< 0.05 vs CTRL).

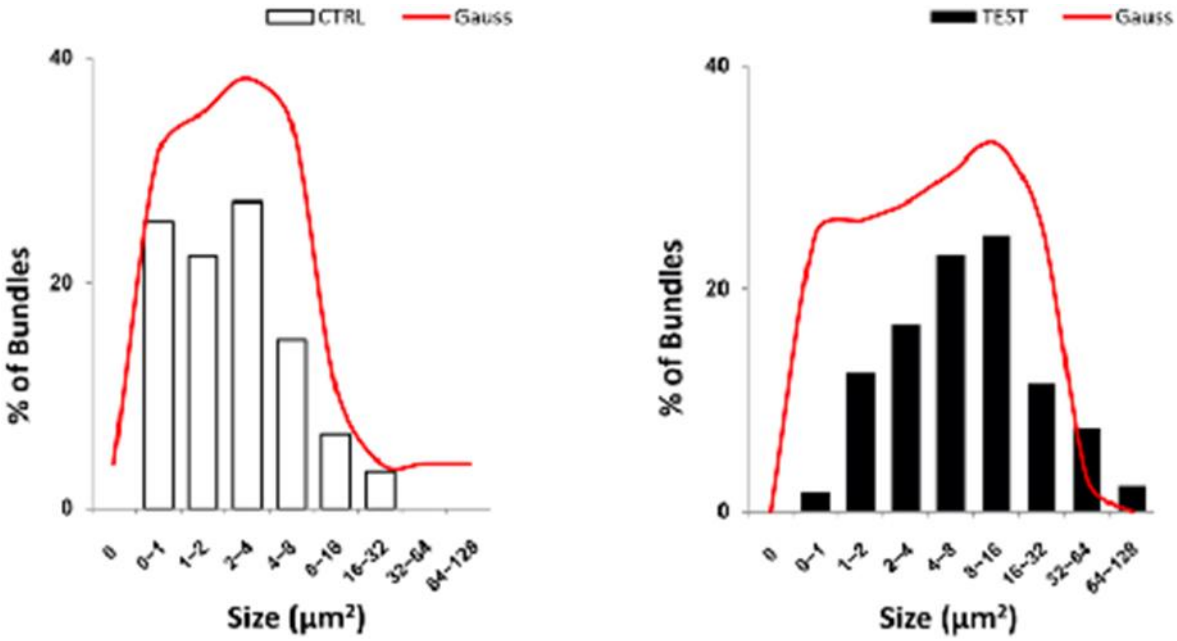

Figure 5. Representative bar and curve plot displaying the distribution frequency of bundle size for both CTRL and TEST groups. The analysis of the distribution frequency of cross- sectional area, i.e., the size of bundles of CTRL and TEST groups, revealed the that most bundles in the CTRL group have an average value of 3.4 ± 4.0, while in the TEST samples, the average is significantly increased to a value of 12.8 ± 16.0. This is also demonstrated by the leftward shift of the CTRL frequency distribution curve compared to the TEST curve

The analysis of the distribution frequency of cross- sectional area, i.e., the size of bundles of CTRL and TEST groups, revealed the that most bundles in the CTRL group have an average value of 3.4 ± 4.0, while in the TEST samples, the average is significantly increased to a value of 12.8 ± 16.0 (Figure 5).

5. ADDITIONAL ULTRA-STRUCTURAL OBSERVATIONS

In addition to the qualitative and quantitative differences described so far, other distinctions have been found between Control and Test specimens. Indeed, it was possible to note the presence of areas characterized by abrupt changes of collagen bundles direction. In cross-sectional images of peri-implant soft tissues, collagen fibers usually appeared as little, small circles closely assembled in bundles of different

sizes (Figures 3 and 4). However, the presence of collagen bundles with longitudinally oriented fibers was occasionally observed (Figure 6).

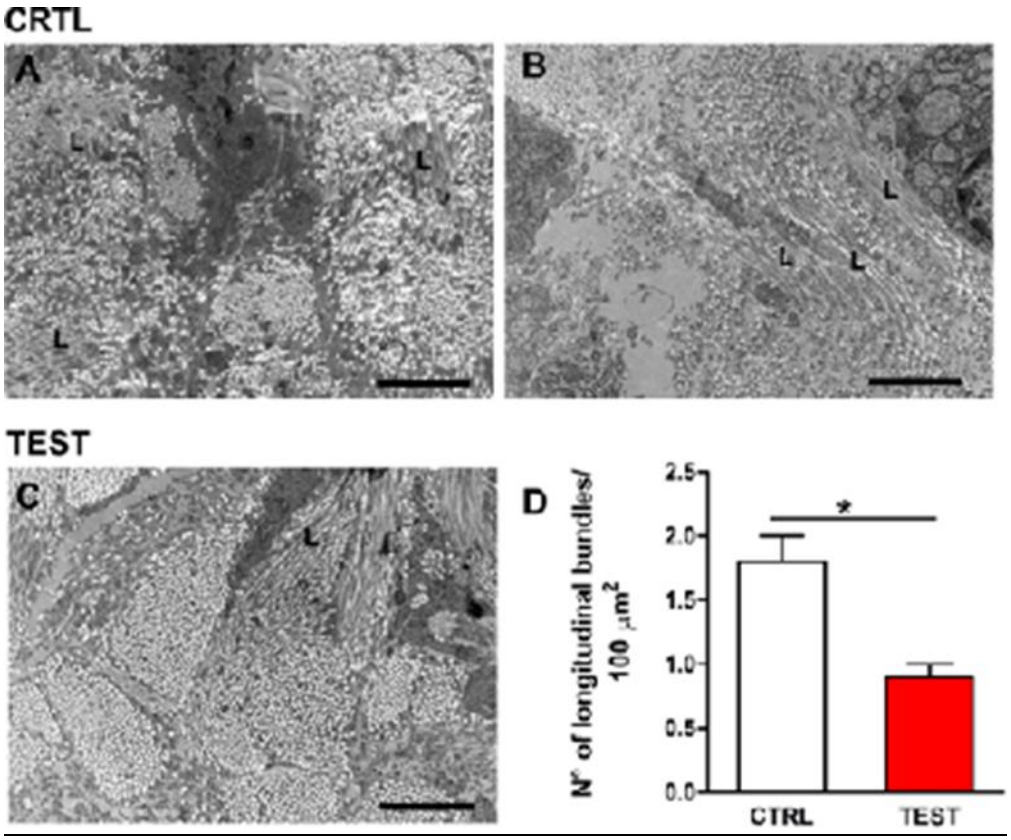

Figure 6. Representative images of different collagen fibers' orientation and appropriately quantitation in (A and B) CTRL and (C) Test samples. In peri-implant cross-sectioned soft tissue, collagen fiber bundles mostly appeared as described in Figure 4. Longitudinal orientation of collagen fibers ("L") was seldom present in both samples, but more frequently in CTRL samples. Scale bars: 2 μm. *$p < 0.05$.

After a careful examination of the specimens, longitudinally oriented fibers appeared different between Control and Test samples. Particularly, in Control specimens (Figures 5A and B), longitudinally oriented collagen fibers ("L") usually assembled in small sized bundles and involved few collagen fibers with a quite random orientation between each other.

In Test specimens, instead, longitudinally oriented collagen fibers ("L") assembled in quite larger bundles involving several, straight, and

parallel-oriented fibers (Figure 5C). The number of longitudinally oriented collagen bundles per 100 mm2 was quantified, and indeed it was found that in Control samples their incidence was significantly higher than in Test samples (Table 3).

	Sample 1	Sample 2	Sample 3	Sample 4
CTRL	1.2 ± 0.3	0.9 ± 0.2	3.4 ± 0.4	1.7 ± 0.2
TEST 1	1.1 ± 0.2	0.8 ± 0.2	1.1 ± 0.3*	0.5 ± 0.2*

Table 3. N° of longitudinal bundles/100 mm2. Data are shown as mean ± SEM (* p< 0.05 vs CTRL).

DISCUSSION

DISCUSSION

1. SUMMARY AND INTERPRETATION OF RESULTS

The geometry of preexisting extracellular matrices or the macro-geometry of the implant might modulate connective tissue cells behavior at the peri-implant mucosa. The hypothesis of the present doctoral thesis was that the morphology of the implant abutment might have triggered a specific alignment of the collagenous network fibers, thus affecting cell polarization, migration, and tensile properties of the tissues.

The macro and micro geometry of the artificial substrate, in this case, the abutment, might provide a contact guidance for the formation of highly polarized capillary-like network. In nature, polarization means to have an organized structure within the ECM, better functionality and, of course, rapid angiogenesis and perfusion in wounded tissues around the healing implant.

The present proof-of-principle animal study compared the peri-implant soft tissue micro anatomy around non-submerged implants with a parallel-walled abutment or with a concave profile abutment inserted in a pig model. The present results demonstrated that the introduction of a concave profile in the abutment led to the organization of a strong wire-shaped connective tissue cuff (about 0.5 mm of thickness) over the implant platform, in which cells, fibrils, and left ECM presented a high degree of anisotropy.

In this way, it has been shown how it is possible to modulate dimensions and the quality of fibers, as well as the morphogenesis of a

highly aligned capillary-like network, by controlling the spatial organization of the neo-formed ECM.

Taken together, these data suggested that during ECM maturation around the abutment interface, the local microenvironment could be influenced by the macroscale tissue geometry, which may trigger long-range signals by inducing internal gradients of mechanical cues, as already reported by other authors [42].

Therefore, tissue geometry acts as both a template and an instructive cue for further morphogenesis. In the present study, the CTRL group with a parallel-walled neck showed a significantly greater ratio of randomly distributed fibers. However, it is well known that moderate crosslinking is beneficial to the mechanical properties of collagen fibers, but excessive crosslinking leads collagen fibers to become more fragile [43].

In the TEST concave group, instead, collagen fibers appeared to be organized in abundant parallel bundles when seen in cross-section and so running circumferentially around the implant when seen from above/axial planes. This result is in line with previous literature describing collagen fiber orientation around implants with a switching platform interface, considered to be an additional “mechanical retention factor” for periodontal fiber orientation [44].

Similarly, studies conducted on other animal models, including monkeys and dogs, have shown a supracrestal circular collagen fiber network that is even comparable to gingival ligaments [27,45].

2. TIES BACK TO THE EXISTING LITERATURE

In a study conducted by Berglundh and Lindhe [24] in 1996 on an animal model, they revealed that a specific level of mucosal thickness is essential for the formation of the supracrestal tissue attachment around dental implants [24].

In the case of deficiency, crestal bone resorption will take place until enough space is created to accommodate both connective tissue and junctional epithelium. Despite their similarity in composition and structure, research has indicated that this attachment apparatus is longer around dental implants when compared to natural dentition, therefore necessitating a greater amount of soft tissue height around implant fixtures [25,46-47].

During recent years, several animal and human reports have described the characteristics, arrangement, and structure of peri-implant soft tissues using different techniques such as light microscopy, polarized light microscopy, scanning electron microscopy (SEM), TEM, and high-resolution X-ray phase-contrast micro-topography (XPCT)[32,40,45,48-49].

As an example, in two animal studies performed more than 30 years ago in monkeys [45,49], it was found that large collagen fiber bundles ran around the implant collar in a parallel way, according to a tangential circular arrangement and converging to form a “circular ring”. TEM findings further showed that these circular fibers appeared to be constituted by bundles of parallel collagen fibrils with a mean diameter of 90 nm, but the inner bundles running close to the metal surface presented a less regular

arrangement; indeed, they had a random course, as well as thinner and different diameters with a mean of 45 nm.

Contrarily, Iezzi et al. [40] in 2021 showed transverse and longitudinal intertwined collagen bundles in a high-resolution XPCT study of peri-implant tissues around human retrieved implants [40]. When evaluating the longitudinal sections, it was found that the closer the fiber bundles were to the metal surface, the more symmetric and regular their direction was. On the other hand, when analyzing transverse bundles of collagen fibers, it was seen a semicircular direction of these bundles, so fibers ran around the abutment, following its circular profile. Similar results were also reported by other researchers.

For instance, in an animal study conducted by Bolle et al. [50], it was found that collagen fibers ran medially toward the healing abutment in a perpendicular direction and the connective tissue was dense, rich in fibroblasts and collagen fibers, which were parallel to the dental implant surface [50].

Other swine studies reported that in some areas, the connective tissue was well organized, while in others, the fibers exhibited a lack of organization, displaying an ambiguous and indistinct orientation [51].

Furthermore, in human studies, a three-dimensional (3D) network of collagen fibers was reported around cone–morse implant connections [40]. Similar results were reported by Mangano et al. [52] using the polarized light and SEM [52]. Collagen fibers were oriented perpendicularly up to a distance of 100 µm from the implant surface, where they became a dense and

chaotic 3D network of parallel fibers running in different directions and an intimate contact of the fibrous matrix with the implant surface was found. After maturation, peri-implant connective tissue had scarce cellularity and blood vessels but became rich in collagen fibers with a few scattered fibroblasts [45].

This structure of the connective tissue has been reported to play a relevant role in the prevention of epithelium down growth and in offering mechanical protection to the osseointegrated part of the implant [53]. The dense 3D framework of the connective tissue bundles determines the mechanical resistance of soft tissues to withstand forces produced during chewing [23]. There is a significant correlation between the degree of fiber orientation in the tissue and its mechanical parameters, such as the elastic modulus.

3. ANSWERS TO THE KNOWLEDGE GAP

Overall, it can be argued that the mechanical environment could play an extremely important role in collagen fiber orientation. It is believed that this phenomenon is caused by an uneven surface shear that gradually attenuated its effect with the distance [54]. The geometry of the artificial substrate might provide contact guidance for the formation of a highly polarized capillary-like network, suggesting clinical applications in triggering fast angiogenesis and perfusion in wounded tissues around the implant [55].

Specifically, collagen fibers can remodel into aligned, anisotropic ensembles under mechanical stimuli, orienting fibers into the direction of

the highest applied strain. Specifically, collagen self-assembly is an entropy-driven process caused by the loss of water between monomers [56]. The goal of the mechanics-mediated fiber orientation experiments is not to recombine the collagen monomer by overcoming the interaction between monomers but to impose additional external forces on the interacting collagen monomer based on the intermolecular interaction, which can lead monomers to bond along the force direction. It can be speculated that, when the distal part of fibers meets the curve perimeter of the abutment concavity, the cellular contraction can generate sufficient force to trigger the aggregation of fibers into bundles.

Other authors believed that the organization of collagen fibers would be mainly dependent on function, namely implant loading [57]. This would lead to the interpretation of radial fibers as a circular ligament around implants. Also, the same authors have demonstrated that this collagen cuff appears to be linked to the periosteum by means of oblique bundles. However, there are no time- dependent studies demonstrating this assumption, nor studies assessing the arrangement of collagen in different rehabilitation designs. In addition, one hypothesis would not exclude the other and vice versa.

It must be remarked that collagen is a well-engineered molecule with native weak points that represent the binding sites for metalloproteinases (MMPs) and bacterial collagenases, a mechanism favoring the regulation of collagen reshaping upon precise stimuli. It has been demonstrated that strain and external loading on fibrils could reinforce collagen in the direction of loading and inhibit the spontaneous formation of entry points

for MMPs, therefore limiting their accessibility and collagen degradation [58].

It follows that directionality and immediate tension on the early wound around implants might control collagen assembly and maturation. Many human tissues are featured by specific alignment patterns involving the ECM of the interstitial connective tissue, stromal cells, and vascular network [59].

Collagen arranged in bundles of aligned fibers controls not only the mechanical properties of tissues, but its density and alignment direction also triggers the polarization of several biological phenomena: cell migration, morphogenesis, vascularization, innervation, tissue regeneration, and wound healing [60]. The anisotropy of the collagen network in tendons controls their mechanical properties and guides the alignment of blood vessels [61]. In any case, having the possibility to control the alignment of a fibroblast-synthetized ECM network still represents a challenge in dentistry.

In 2011, Caliari & Harley [62] pointed out that “a range of studies have suggested that successful regeneration templates for natively aligned tissues must provide tissue-specific aligned contact guidance cues that recapitulate aspects of the tissue anisotropy" [62]. As discussed in the proof of principle study of the present doctoral thesis, including a groove in the abutment would mean recapitulating aspects of the dental anatomy, thus providing a stable chamber for supra-crestal collagen fibers arrangement.

Collagen I fibers - the most common in the periodontium and in the peri-implant mucosa - can remodel into aligned (anisotropic) ensembles

under mechanical stimuli, with fibers orienting themselves along the direction of the highest applied strain [63]. Anisotropic fibers have significant biological relevance and influence the degree of cell-substrate contact, induce cell polarization, and guide cell motility [64].

Collagen in the ECMs undergoes remodeling by fibroblasts which establish an adhesion receptor mediated tension on ECM [65]. The complex interplay between fibroblasts and their own synthesized collagen network results in different tissues organization, composition and texture providing a wide spectrum of specialized functions [56].

Moreover, the fibroblasts-synthesized collagen network serves as scaffold to which other extracellular components can connect (i.e. fibronectin, and glycosaminoglycans) forming a complex structure controlling cell fate and tissue function by means of different biophysical mechanisms: fibers organization (isotropic vs. anisotropic), fiber thickness, spatial and temporal release/presentation of growth factors and peptide mediators [66]. Having the possibility to control the alignment of a fibroblast-synthesized ECM network is still a challenge.

The presence of exogenous components, acting as ECM surrogates, as the implant and prosthetic components would be, still represents a limit toward the physiological mimicry of the corresponding teeth. Efforts in the design of scaffolds able to prevent contraction - mediated by myofibroblasts - have been made.

In the present study, using a deep groove in the abutment collar, it was possible to obtain a 1,5 mm wide connective tissue structure, in which

cells and their own extracellular matrix showed a high degree of anisotropy. The present study showed also that, by controlling the spatial organization of the newly-formed extracellular matrix, it was possible to modulate the dimension and quality of the fibers and the morphogenesis of a highly aligned capillary-like network.

There is a significant correlation between the degree of fiber orientation in the tissue and its mechanical parameters such as elastic modulus. It can be argued that the mechanical environment could play an extremely important role in collagen fiber orientation. It is believed that this phenomenon is caused by uneven surface shear, that is, the shear action of the round surface is gradually attenuated with distance.

Collagen self-assembly is an entropy-driven process caused by the loss of water between monomers, and the self-assembly process is mainly divided into two stages: nucleation and growth. Based on electrostatic interaction and hydrophobic interaction, the C-terminal peptides of collagen monomers bind to specific binding sites of other collagen monomers to form microfibers, and the change of ionic strength and pH value can affect the interaction between molecules [67].

In addition, the goal of the mechanics-mediated fiber orientation experiments is not to recombine the collagen monomer by overcoming of the interaction between the monomers, but to impose additional external force on the interacting collagen monomer on the basis of the intermolecular interaction, which can cause the monomers to bond along the direction of force. It can be hypothesized that, when the distal end of the fibers contacts with the curve perimeter of the abutment groove, the

cellular contraction can generate sufficient force to cause the fibers to aggregate into bundles. It is also known that, during this process, the decorin secreted by cells inhibited the occurrence of cross-linking, and the fibers were, then, loosely arranged.

CONCLUSIONS

CONCLUSIONS

In conclusion, within the limitations of the present study due to the use of a small number of animals and implants that might bring uncertainty and risk to the research results:

1. The present study on the peri-implant connective tissue structure evaluated by histological and TEM analysis showed that the concave transmucosal design could favor the deposition and growth of the connective tissue.

2. This concavity generated a significant amount of connective tissue in the early healing phase, increased the thickness of this circular peri-implant network, and promoted the convergence of collagen fibers toward the abutment collar with the formation of a wide circular collagen structure over the implant platform.

3. As fiber anisotropy is a defining feature in highly specialized tissues, it is important at the ISC as well.

4. Starting from this proof-of-principle animal study, future research involving a larger number of animals and implants, as well as using other mechanical detection methods together with histological and TEM analysis, will be necessary to confirm and strengthen the present results.

REFERENCES

REFERENCES

1. Moraschini V, Poubel LA, Ferreira VF, Barboza Edos S. Evaluation of survival and success rates of dental implants reported in longitudinal studies with a follow-up period of at least 10 years: a systematic review. Int J Oral Maxillofac Surg 2015; 44:377-388.

2. Barone A, Marconcini S, Giammarinaro E, Mijiritsky E, Gelpi F, Covani U. Clinical outcomes of implants placed in extraction sockets and immediately restored: a 7-year single-cohort prospective study. Clin Implant Dent Relat Res 2016;18:1103-1112.

3. Albrektsson T, Brånemark PI, Hansson HA, Lindström J. Osseointegrated titanium implants. Requirements for ensuring a long-lasting, direct bone-to-implant anchorage in man. Acta Orthop Scand 1981; 52:155-70.

4. Geckili O, Bilhan H, Geckili E, Cilingir A, Mumcu E, Bural C. Evaluation of possible prognostic factors for the success, survival, and failure of dental implants. Implant Dent. 2014; 23:44-50.

5. Schwarz F, Ramanauskaite A. It is all about peri-implant tissue health. Periodontol 2000 2022; 88:9–12.

6. Suárez-López Del Amo F, Lin GH, Monje A, Galindo-Moreno P, Wang HL. Influence of soft tissue thickness on peri-implant marginal bone loss: a systematic review and meta-analysis. J Periodontol 2016; 87:690-699.

7. Ivanovski S, Lee R. Comparison of peri-implant and periodontal marginal soft tissues in health and disease. Periodontol 2000. 2018;76:116-130.

8. Mattheos N, Vergoullis I, Janda M, Miseli A. The Implant Supracrestal Complex and its significance for long-term successful clinical outcomes. Int J Prosthodont 2021; 34:88-100.

9. Hämmerle CH, Chen ST, Wilson TG Jr. Consensus statements and recommended clinical procedures regarding the placement of implants in extraction sockets. Int J Oral Maxillofac Implants. 2004;19 Suppl:26-28.

10. Atieh M.A, Payne A.G, Duncan W.J, de Silva R.K, Cullinan M.P. Immediate placement or immediate restoration/loading of single implants for molar tooth replacement: a systematic review and meta-analysis. Int J Oral Maxillofac Implants 2010; 25:401–415.

11. Pitman J, Seyssens L, Christiaens V, Cosyn J. Immediate implant placement with or without immediate provisionalization: A systematic review and meta-analysis. J Clin Periodontol. 2022 Oct;49(10):1012-1023. doi: 10.1111/jcpe.13686. Epub 2022 Jul 15. PMID: 35734911.

12. Marconcini S, Giammarinaro E, Derchi G, Alfonsi F, Covani U, Barone A. Clinical outcomes of implants placed in ridge-preserved versus nonpreserved sites: A 4-year randomized clinical trial. Clin Implant Dent Relat Res. 2018 Dec;20(6):906-914.

13. Seyssens L, De Lat L, Cosyn J. Immediate implant placement with or without connective tissue graft: A systematic review and meta-analysis. J Clin Periodontol 2021;48:284-301.

14. Ruales-Carrera E, Pauletto P, Apaza-Bedoya K, Volpato CAM, Özcan M, Benfatti CAM. Peri- implant tissue management after immediate implant placement using a customized healing abutment. J Esthet Restor Dent. 2019; 31:533-541.

15. Velasco-Ortega E, Cracel-Lopes JL, Matos Garrido N, Jiménez-Guerra A, Ortiz-Garcia I, Moreno-Muñoz J, et al. Immediate loading with fixed totally rehabilitation of implants placed in periodontal patients. Int J Environ Res Public Health 2022, 19, 13162.

16. Slagter KW, Raghoebar GM, Hentenaar DFM, Vissink A, Meijer HJA. Immediate placement of single implants with or without immediate provisionalization in the maxillary aesthetic region: A 5-year comparative study. J Clin Periodontol 2021;48:272-283.

17. Ferrantino L, Camurati A, Gambino P, Marzolo M, Trisciuoglio D, Santoro G, Farina V, Fontana F, Asa'ad F, Simion M. Aesthetic outcomes of non-functional immediately restored single post-extraction implants with and without connective tissue graft: A multicentre randomized controlled trial. Clin Oral Implants Res 2021;32:684-694.

18. Bolle C, Gustin MP, Fau D, Exbrayat P, Boivin G, Grosgogeat B. Early periimplant tissue healing on 1-piece implants with a concave transmucosal design: a histomorphometric study in dogs. Implant Dent 2015; 24:598-606.

19. Tomasi C, Tessarolo F, Caola I, Wennström J, Nollo G, Berglundh T. Morphogenesis of peri- implant mucosa revisited: An experimental study in humans. Clin Oral Implants Res 2014; 25:997–1003.

20. Parpaiola A, Cecchinato D, Toia M, Bressan E, Speroni S, Lindhe J. Dimensions of the healthy gingiva and peri-implant mucosa. Clin Oral Impl Res 2015; 26:657-662.

21. Glauser R, Schüpbach P, Gottlow J, Hämmerle CH. Periimplant soft tissue barrier at experimental one-piece mini-implants with different surface topography in humans: A light- microscopic overview and histometric analysis. Clin Implant Dent Relat Res 2005;7 Suppl 1: S44-51.

22. Piattelli A, Scarano A, Piattelli M, Bertolai R, Panzoni E Histologic aspects of the bone and soft tissues surrounding three titanium non-submerged plasma-sprayed implants retrieved at autopsy: a case report J Periodontol 1997;68:694-700.

23. Romanos GE, Traini T, Johansson CB, Piattelli A Biologic width and morphologic characteristics of soft tissues around immediately loaded implants: studies performed on human autopsy specimens. J Periodontol 2010; 81:70-78.

24. Berglundh T, Lindhe J. Dimension of the periimplant mucosa. Biological width revisited. J Clin Periodontal 1996;23: 971-973.

25. AbrahamssonI, BerglundhT, Wennstrom J, Lindhe J. The peri-implant hard and soft tissues at different implant systems. A comparative study in the dog. Clin Oral Implants Res 1996; 7:212-219.

26. Sculean A, Gruber R, Bosshardt DD. Soft tissue wound healing around teeth and dental implants. J Clin Periodontol 2014;41 Suppl 15: S6-22.

27. Rodríguez X, Navajas A, Vela X, Fortuño A, Jimenez J, Nevins M. Arrangement of peri- implant connective tissue fibers around platform-switching implants with conical abutments and its relationship to the underlying bone: a human histologic study. Int J Perio Restor Dent 2016; 36:533-540.

28. Bishti S, Strub JR, Wael Att W Effect of the implant–abutment interface on peri-implant tissues: A systematic review. Acta Odont Scand 2014; 72: 13–25.

29. Rompen E, Domken O, Degidi M, Farias Pontes AE, Piattelli A. The effect of material characteristics, of surface topography and of implant components and connections on soft tissue integration: a literature review. Clin Oral Implants Res 2006;17 Suppl 2:55-67.

30. Chien, H.H.; Schroering, R.L.; Prasad, H.S.; Tatakis, D.N. Effects of a new implant abutment design on peri-implant soft tissues. J. Oral Implantol. 2014, 40, 581–588.

31. Huh JB, Rheu GB, Kim YS, Jeong CM, Lee JY, Shin SW Influence of implant transmucosal design on early peri-implant tissue responses in beagle dogs. Clin Oral Implants Res. 2014; 25:962-8.

32. Delgado-Ruiz RA, Calvo-Guirado JL, Abboud M, Ramirez-Fernandez MP, Maté-Sánchez de Val JE, Negri B, Gomez-Moreno G, Markovic A. Connective tissue characteristics around healing abutments of different geometries: new methodological technique under circularly polarized light. Clin Implant Dent Relat Res 2015; 17:667-680.

33. Lang, N.P., Pun, L., Lau, K.Y., Li, K.Y. & Wong, M.C. A systematic review on survival and success rates of implants placed immediately into fresh extraction sockets after at least 1 year. Clin Oral Impl Res 2012; 23(Suppl. 5): 39–66.

34. Araujo, M.G. & Lindhe, J. Dimensional ridge alterations following tooth extraction. An experimental study in the dog. J Clin Periodontol 2005; 32: 212–218.

35. Lazzara, R.J. & Porter, S.S. Platform switching: a new concept in implant dentistry for controlling postrestorative crestal bone levels. Int J Perio Rest Dent 2006; 26: 9–17.

36. Hammerle CHF, Tarnow D. The etiology of hard- and soft-tissue deficiencies at dental implants: a narrative review. J Clin Periodontol 2018;45(Suppl 20): S267-S277.

37. Thoma DS, Naenni N, Figuero E, et al. Effects of soft tissue augmentation procedures on peri- implant health or disease: a systematic review and meta-analysis. Clin Oral Implants Res. 2018;29(Suppl 15):32-49.

38. Tavelli L, Barootchi S, Avila-Ortiz G, Urban IA, Giannobile WV, Wang HL. Peri-implant soft tissue phenotype modification and its impact on peri-implant health: a systematic review and network meta-analysis. J Periodontol 2021;92(1):21-44.

39. du Sert, N.P.; Hurst, V.; Ahluwalia, A.; Alam, S.; Avey, M.T.; Baker, M.; Browne, W.J.; Clark, A.; Cuthill, I.C.; Dirnagl, U.; et al. The

REFERENCES

ARRIVE Guidelines 2.0: Updated Guidelines for Reporting Animal Research. PLoS Biol 2020, 18.

40. Iezzi, G.; Di Lillo, F.; Furlani, M.; Degidi, M.; Piattelli, A.; Giuliani, A. The Symmetric 3D organization of connective tissue around implant abutment: a key-issue to prevent bone resorption. Symmetry 2021, 13, 1126.

41. Boncompagni, S.; Rossi, A.E.; Micaroni, M.; Beznoussenko, G.V.; Polishchuk, R.S.; Dirksen, R.T.; Protasi, F. Mitochondria Are Linked to Calcium Stores in Striated Muscle by Developmentally Regulated Tethering Structures. Mol. Biol. Cell 2009, 20, 1058–1067.

42. Nelson, C.M. Geometric Control of Tissue Morphogenesis. Biochim Biophys Acta 2009, 1793, 903–910, doi:10.1016/J.BBAMCR.2008.12.014.

43. Buehler, M.J. Nature Designs Tough Collagen: Explaining the Nanostructure of Collagen Fibrils. Proc. Natl. Acad. Sci. USA 2006, 103, 12285–12290.

44. Ciurana, X.; Acedo, Á.; Vela, X.; Fortuño, A.; García, J.; Nevins, M. Arrangement of Peri- Implant Connective Tissue Fibers Around Platform-Switching Implants with Conical Abutments and Its Relationship to the Underlying Bone: A Human Histologic Study. Int. J. Periodontics Restor. Dent. 2016, 36, 533–540.

45. Ruggeri, A.; Franchi, M.; Marini, N.; Trisi, P.; Piattelli, A. Supracrestal Circular Collagen Fiber Network around Osseointegrated Nonsubmerged Titanium Implants. Clin. Oral Implant. Res. 1992, 3, 169–175.

46. Abrahamsson, I.; Berglundh, T.; Moon, I.S.; Lindhe, J. Peri-implant tissues at submerged and non-submerged titanium implants. J. Clin. Periodontol. 1999, 26, 600–607.

47. Berglundh, T.; Lindhe, J.; Ericsson, I.; Marinello, C.P.; Liljenberg, B.; Thomsen, P. The soft tissue barrier at implants and teeth. Clin. Oral Implant. Res. 1991, 2, 81–90.

48. Giuliani, A.; Cedola, A. Advanced high-resolution tomography in regenerative medicine; Springer: Berlin/Heidelberg, Germany, 2018.

49. Ruggeri, A.; Franchi, M.; Trisi, P.; Piattelli, A. Histologic and ultrastructural findings of gingival circular ligament surrounding osseointegrated nonsubmerged loaded titanium implants. Int. J. Oral Maxillofac. Implant. 1994, 9, 636–643.

50. Bolle, C.; Gustin, M.-P.; Fau, D.; Boivin, G.; Exbrayat, P.; Grosgogeat, B. Soft tissue and marginal bone adaptation on platform-switched implants with a morse cone connection: a histomorphometric study in dogs. Int. J. Periodontics Restor. Dent. 2016, 36, 221–228Z

51. Tetè, S.; Mastrangelo, F.; Bianchi, A.; Zizzari, V.; Scarano, A. Collagen fiber orientation around machined titanium and zirconia dental implant necks: an animal study. Int. J. Oral Maxillofac. Implant. 2009, 24, 52–58.

52. Mangano, C.; Piattelli, A.; Scarano, A.; Raspanti, M.; Shibli, J.; Mangano, F.; Perrotti, V.; Iezzi, G. A light and scanning electron microscopy study of human direct laser metal forming dental implants. Int. J. Periodontics Restor. Dent. 2014, 34, 9–17.

53. Cui X, Reason T, Pardi V, Wu Q, Martinez Luna AA. CBCT analysis of crestal soft tissue thickness before implant placement and its relationship with cortical bone thickness. BMC Oral Health. 2022; 22:593.

54. Lin, J.; Shi, Y.; Men, Y.; Wang, X.; Ye, J.; Zhang, C. Mechanical roles in formation of oriented collagen fibers. Tissue Eng. Part B Rev. 2020; 26: 116–128.

55. Casale, C.; Imparato, G.; Mazio, C.; Netti, P.A.; Urciuolo, F. Geometrical confinement controls cell, ecm and vascular network alignment during the morphogenesis of 3D bioengineered human connective tissues. Acta Biomater 2021; 131: 341–354.

56. Sun, B. The mechanics of fibrillar collagen extracellular matrix. Cell Rep Phy Sci 2021, 2.

57. Schierano, G.; Ramieri, G.; Cortese, M.G.; Aimetti, M.; Preti, G. Organization of the connective tissue barrier around long-term loaded implant abutments in man. Clin. Oral Implant Res 2002; 13: 460–464.

58. Birk, D.E.; Nurminskaya, M.V.; Zycband, E.I. Collagen fibrillogenesis in situ: fibril segments undergo post-depositional modifications resulting in linear and lateral growth during matrix development. Dev Dyn 1995; 202: 229–243.

59. Yang, G.; Mahadik, B.; Choi, J.Y.; Fisher, J.P. Vascularization in tissue engineering: fundamentals and state-of-art. Prog Biomed Eng 2020; 2: 012002.

60. Saeidi, N.; Karmelek, K.P.; Paten, J.A.; Zareian, R.; DiMasi, E.; Ruberti, J.W. Molecular crowding of collagen: a pathway to produce

highly-organized collagenous structures. Biomaterials 2012; 33: 7366–7374.

61. Silver FH, Freeman JW, Seehra GP. Collagen self-assembly and the development of tendon mechanical properties. J Biomech 2003; 36:1529-1553.

62. Caliari, S.R., and Harley, B.A.C. The effect of anisotropic collagen-GAG scaffolds and growth factor supplementation on tendon cell recruitment, alignment, and metabolic activity. Biomaterials 2011; 32: 5330.

63. Marchand M, Monnot C, Muller L, Germain S. Extracellular matrix scaffolding in angiogenesis and capillary homeostasis. Semin Cell Dev Biol 2019;89:147-156.

64. Schwarz F, Ramanauskaite A. It is all about peri-implant tissue health. Periodontol 2000 2022; 88:9-12.

65. Nelson CM. Geometric control of tissue morphogenesis. Biochim Biophys Acta 2009;1793: 903-910.

66. Glass-Brudzinski J, Perizzolo D, Brunette DM. Effects of substratum surface topography on the organization of cells and collagen fibers in collagen gel cultures. J Biomed Mater Res 2002; 61:608-618.

67. Buehler, M.J. Nature designs tough collagen: explaining the nanostructure of collagen fibrils. Proc Natl Acad Sci USA 2006; 103: 12285–12290 .

CURRICULUM VITAE

CURRICULUM VITAE

Academic records

ENRICA GIAMMARINARO

Date of birth 20/04/1989, Mazara del Vallo (TP), Italy. ORCID: 0000-0001-8398-8525

Seville University, Dentistry Department, EV ORTEGA

Sept 2022 - Sept. 2023

- PhD Candidate.

Valencia University, MD PENARROCHA

2016 – 2019

- Fellow Researcher.

Instituto Stomatologico Toscano, Lido di Camaiore (Italy)

2014 – ongoing

- Fellow Researcher.

Università degli Studi di Siena, (Siena, Italy)

2020 - ongoing

- Oral Surgery Residence

Università degli Studi di Pisa, (Pisa, Italy)

2008 - 2014

- Master Degree in Dentistry

Publications discussed in the present doctoral thesis

Covani U, Giammarinaro E, Di Pietro N, Boncompagni S, Rastelli G, Romasco T, Velasco- Ortega E, Jimenez-Guerra A, Iezzi G, Piattelli A, Marconcini S. Electron Microscopy (EM) Analysis of Collagen Fibers in the Peri-Implant Soft Tissues around Two Different Abutments. J Funct Biomater. 2023 Aug 29;14(9):445. doi: 10.3390/jfb14090445. PMID: 37754859; PMCID: PMC10532031.

All publications:

1.Covani U, Giammarinaro E, Di Pietro N, Boncompagni S, Rastelli G, Romasco T, Velasco-Ortega E, Jimenez-Guerra A, Iezzi G, Piattelli A, Marconcini S. Electron Microscopy (EM) Analysis of Collagen Fibers in the Peri-Implant Soft Tissues around Two Different Abutments. J Funct Biomater. 2023 Aug 29;14(9):445. doi: 10.3390/ jfb14090445. PMID: 37754859; PMCID: PMC10532031.

2. Enrica Giammarinaro, Ugo Covani, Eugenio Velasco-Ortega, Simone Marconcini, Immediate implant and simultaneous buccal bone reconstruction with a composite graft of calcium sulfate and leukocyte-platelet-rich fibrin. A one-year case report, Oral and Maxillofacial Surgery Cases, Volume 9, Issue 3, 2023, 100331, ISSN 2214-5419, https:// doi.org/10.1016/j.omsc.2023.100331.

3. Cosola S, Oldoini G, Giammarinaro E, Covani U, Genovesi A, Marconcini S. The effectiveness of the information-motivation model and

domestic brushing with a hypochlorite-based formula on peri-implant mucositis: A randomized clinical study. Clin Exp Dent Res. 2021 Oct 22. doi: 10.1002/cre2.487. Epub ahead of print. PMID: 34677005.

4. Rigo L, Tolardo J, Giammarinaro E, Covani U, Caso G. Fully Guided Zygomatic Implant Surgery. J Craniofac Surg. 2021 Jul 27. doi:10.1097/SCS.0000000000008005. Epub ahead of print. PMID: 34320580.

5. Marconcini S, Giammarinaro E, Cosola S, Oldoini G, Genovesi A, Covani U. Effects of Non-Surgical Periodontal Treatment on Reactive Oxygen Metabolites and Glycemic Control in Diabetic Patients with Chronic Periodontitis. Antioxidants (Basel). 2021 Jun 30;10(7):1056. doi: 10.3390/antiox10071056. PMID: 34208802; PMCID: PMC8300765.

6. Cosola S, Kim YS, Park YM, Giammarinaro E, Covani U. Coronectomy of Mandibular Third Molar: Four Years of Follow-Up of 130 Cases. Medicina (Kaunas). 2020 Nov 27;56(12):654. doi: 10.3390/medicina56120654. PMID: 33261207; PMCID: PMC7760348.

7. Covani U, Giammarinaro E, Marconcini S. A New Approach for Lateral Sinus Floor Elevation. J Craniofac Surg. 2020 Nov/Dec;31(8):2320-2323. doi: 10.1097/ SCS.0000000000006766. PMID: 33136881.

8. Marconcini S, Giammarinaro E, Covani U. The timeliness of ozone in the COVID era. Eur Rev Med Pharmacol Sci. 2020 May;24(9):4625-4626. doi: 10.26355/eurrev_202005_21146. PMID: 32432725.

9. Covani U, Giammarinaro E, Marconcini S. Alveolar socket remodeling: The tug-of-war model. Med Hypotheses. 2020 Sep;142:109746. doi:10.1016/j.mehy.2020.109746. Epub 2020 Apr 20. PMID: 32344287.

10. Menchini-Fabris GB, Marconcini S, Giammarinaro E, Barone A, Toti P, Covani U. Extension implants in the atrophic posterior maxilla: 1-year results of a retrospective case-series. J Dent Sci. 2020 Mar;15(1):9-13. doi: 10.1016/j.jds.2018.11.009. Epub 2020 Jan 6. PMID: 32256994; PMCID: PMC7109493.

11. Oldoini G, Frabattista GR, Saragoni M, Cosola S, Giammarinaro E, Genovesi AM, Marconcini S. Ozone Therapy for Oral Palatal Ulcer in a Leukaemic Patient. Eur J Case Rep Intern Med. 2020 Jan 14;7(2):001406. doi: 10.12890/2020_001406. PMID: 32133312; PMCID: PMC7050963.

12. Giammarinaro E, Cosola S, Oldoini G, Gulia F, Peñarrocha-Oltra D, Marconcini S, Genovesi AM. Local Formula with Mucoadhesive Property: A Randomized Clinical Trial of a Therapeutic Agent for the Treatment of Oral Aphthous Ulcers. J Contemp Dent Pract. 2019 Nov 1;20(11):1249-1253. PMID: 31892674.

13. Marconcini S, Giammarinaro E, Cosola S, Genovesi AM, Covani U. Mandibular Osteonecrosis Associated with Antacid Therapy (Esomeprazole). Eur J Case Rep Intern Med. 2019 Oct 14;6(10):001279. doi: 10.12890/2019_001279. PMID: 31742205; PMCID: PMC6822666.

14. Marconcini S, Denaro M, Cosola S, Gabriele M, Toti P, Mijiritsky E, Proietti A, Basolo F, Giammarinaro E, Covani U. Myofibroblast Gene Expression Profile after Tooth Extraction in the Rabbit. Materials (Basel). 2019 Nov 9;12(22):3697. doi: 10.3390/ ma12223697. PMID: 31717520; PMCID: PMC6888118.

15. Marconcini S, Giammarinaro E, Covani U, Mijiritsky E, Vela X, Rodríguez X. The Effect of Tapered Abutments on Marginal Bone Level: A Retrospective Cohort Study. J Clin Med. 2019 Aug 24;8(9):1305. doi: 10.3390/jcm8091305. PMID: 31450607; PMCID: PMC6780335.

16. Marconcini S, Goulding M, Oldoini G, Attanasio C, Giammarinaro E, Genovesi A. Clinical and patient-centered outcomes post non-surgical periodontal therapy with the use of a non-injectable anesthetic product: A randomized clinical study. J Investig Clin Dent. 2019 Nov;10(4):e12446. doi: 10.1111/jicd.12446. Epub 2019 Jul 28. PMID: 31353819; PMCID: PMC6899940.

17. Cosola S, Giammarinaro E, Marconcini S, Lelli M, Lorenzi C, Genovesi AM. Prevention of bacterial colonization on suture threads after oral surgery: comparison between propolis- and chlorhexidine-based formulae. J Biol Regul Homeost Agents. 2019 Jul- Aug;33(4):1275-1281. PMID: 31298019.

18. Cosola S, Giammarinaro E, Genovesi AM, Pisante R, Poli G, Covani U, Marconcini S. A short-term study of the effects of ozone irrigation in an orthodontic population with fixed appliances. Eur J Paediatr Dent. 2019 Mar;20(1):15-18. doi: 10.23804/ejpd.2019.20.01.03. PMID: 30919638.

19. Marconcini S, Covani U, Giammarinaro E, Velasco-Ortega E, De Santis D, Alfonsi F, Barone A. Clinical Success of Dental Implants Placed in Posterior Mandible Augmented With Interpositional Block Graft: 3-Year Results From a Prospective Cohort Clinical Study. J Oral Maxillofac Surg. 2019 Feb;77(2):289-298. doi: 10.1016/j.joms.2018.09.031. Epub 2018 Oct 4. PMID: 30712534.

20. Crespi R, Marconcini S, Crespi G, Giammarinaro E, Menchini Fabris GB, Barone A, Covani U. Nonsurgical Treatment of Peri-implantitis Without Eliminating Granulation Tissue: A 3-Year Study. Implant Dent. 2019 Feb;28(1):4-10. doi: 10.1097 ID.0000000000000832. PMID: 30363048.

21. Marconcini S, Giammarinaro E, Derchi G, Alfonsi F, Covani U, Barone A. Clinical outcomes of implants placed in ridge-preserved versus nonpreserved sites: A 4-year randomized clinical trial. Clin Implant Dent Relat Res. 2018 Dec;20(6):906-914. doi: 10.1111/cid.12682. Epub 2018 Oct 11. PMID: 30307130.

22. Giammarinaro E, Marconcini S, Genovesi A, Poli G, Lorenzi C, Covani U. Propolis as an adjuvant to non-surgical periodontal treatment: a clinical study with salivary anti-oxidant capacity assessment. Minerva Stomatol. 2018 Oct;67(5):183-188. doi: 10.23736/ S0026-4970.18.04143-2. PMID: 30182639.

23. Cosola S, Marconcini S, Giammarinaro E, Poli GL, Covani U, Barone A. Oral health- related quality of life and clinical outcomes of immediately or delayed loaded implants in the rehabilitation of edentulous

jaws: a retrospective comparative study. Minerva Stomatol. 2018 Oct;67(5):189-195. doi: 10.23736/S0026-4970.18.04134-1. Epub 2018 Apr 16. PMID: 29660976.

24. Marconcini S, Giammarinaro E, Toti P, Alfonsi F, Covani U, Barone A. Longitudinal analysis on the effect of insertion torque on delayed single implants: A 3-year randomized clinical study. Clin Implant Dent Relat Res. 2018 Jun;20(3):322-332. doi: 10.1111/ cid.12586. Epub 2018 Jan 23. PMID: 29359880.

25. Menchini Fabris GB, Gelpi F, Giammarinaro E, Velasco Ortega E, Marconcini S, Covani U. A novel CAD/CAM-based surgical template for mandibular osteoplasty and guided implant insertion. J Biol Regul Homeost Agents. 2017 APR-JUN;31(2 Suppl. 2):99-106. PMID: 28702970.

26. Barone A, Marconcini S, Giammarinaro E, Mijiritsky E, Gelpi F, Covani U. Clinical Outcomes of Implants Placed in Extraction Sockets and Immediately Restored: A 7-Year Single-Cohort Prospective Study. Clin Implant Dent Relat Res. 2016 Dec;18(6):1103-1112. doi: 10.1111/cid.12393. Epub 2016 Feb 16. PMID: 26888632.

27. AM Genovesi, S Marconcini, M Lelli, E Giammarinaro, A Barone. In Vitro Comparison of Three Desensitizing Prophylaxis Pastes: A Morphological Analysis, J Oral Hyg Health 3 (186), 2332- 0702.1000186

28. Marconcini, S., Giammarinaro, E., Giampietro, O., Giampietro, C., Soder, B., Rdh, A. G., ... & Covani, U. Oxidative stress and periodontal disease in diabetic patients: a 3- month pilot study.

29. Toti P, Marconcini S, Giammarinaro E, Pedretti G, Barone A, Covani U. The Influence of Prosthesis Design on the Outcomes of Tooth Implants Immediately Placed and Loaded by Means of One-Piece Titanium Machined Restoration. J Oral Implantol. 2018 Apr;44(2):87-93. doi: 10.1563/ aaid-joi-D-17-00152. Epub 2017 Nov 28. PubMed PMID: 29182488.

30. Marconcini S, Giammarinaro E, Covani U, Mascolo A, Caso G, Del Corso M. Immediate restoration of fixed full-arch prostheses placed on implants in both fresh and healed sockets using the flat one-bridge technique: a 7-year retrospective study. BMC Oral Health. 2021 Dec 3;21(1):617. doi: 10.1186/s12903-021-01988-0. PMID: 34861877; PMCID: PMC8642953.

Journal of *Functional Biomaterials*

MDPI

Article

Electron Microscopy (EM) Analysis of Collagen Fibers in the Peri-Implant Soft Tissues around Two Different Abutments

Ugo Covani [1,†], Enrica Giammarinaro [1,†], Natalia Di Pietro [2,3,*,†], Simona Boncompagni [3,4], Giorgia Rastelli [3,4], Tea Romasco [2,3], Eugenio Velasco-Ortega [5], Alvaro Jimenez-Guerra [5], Giovanna Iezzi [2], Adriano Piattelli [6,7] and Simone Marconcini [1]

1 Department of Stomatology, Tuscan Dental Institute, 55041 Lido di Camaiore, Italy; covani@covani.it (U.C.); e.giammarinaro@gmail.com (E.G.); simosurg@gmail.com (S.M.)
2 Department of Medical, Oral and Biotechnological Sciences, "G. d'Annunzio" University of Chieti-Pescara, 66013 Chieti, Italy; tea.romasco@unich.it (T.R.); gio.iezzi@unich.it (G.I.)
3 Center for Advanced Studies and Technology—CAST, "G. d'Annunzio" University of Chieti-Pescara, 66013 Chieti, Italy; simona.boncompagni@unich.it (S.B.); giorgia.rastelli@unich.it (G.R.)
4 Department of Neuroscience, Imaging and Clinical Sciences, "G. d'Annunzio" University of Chieti-Pescara, 66013 Chieti, Italy
5 Department of Stomatology, Faculty of Dentistry, University of Seville, 41013 Seville, Spain; evelasco@us.es (E.V.-O.); alopajanosas@hotmail.com (A.J.-G.)
6 School of Dentistry, Saint Camillus International University of Health and Medical Sciences, 00131 Rome, Italy; apiattelli51@gmail.com
7 Facultad de Medicina, UCAM Universidad Católica San Antonio de Murcia, 30107 Murcia, Spain
* Correspondence: natalia.dipietro@unich.it
† These authors contributed equally to this work.

Abstract: The design of the implant prosthesis–abutment complex appears crucial for shaping healthy and stable peri-implant soft tissues. The aim of the present animal study was to compare two implants with different healing abutment geometries: a concave design (TEST) and a straight one (CTRL). Transmission electron microscopy (TEM) was used to quantify the three-dimensional topography and morphological properties of collagen at nanoscale resolution. Two swine were included in the experiment and six implants per animal were randomly placed in the left or right hemimandible in either the physiologically mature bone present between the lower canine and first premolar or in the mandibular premolar area. Each CTRL implant was positioned across from its respective TEST implant on the other side of the jaw. After 12 weeks of healing, eight specimens (four CTRL and four TEST) were retrieved and prepared for histological and TEM analysis. The results showed a significantly higher percentage of area covered by collagen bundles and average bundle size in TEST implants, as well as a significant decrease in the number of longitudinally oriented bundles with respect to CTRL implants, which is potentially due to the larger size of TEST bundles. These data suggest that a concave transmucosal abutment design serves as a scaffold, favoring the deposition and growth of a well-organized peri-implant collagen structure over the implant platform in the early healing phase, also promoting the convergence of collagen fibers toward the abutment collar.

Keywords: collagen fibers; concave abutment; healing abutment; peri-implant soft tissues; swine; ultrastructural analysis

Citation: Covani, U.; Giammarinaro, E.; Di Pietro, N.; Boncompagni, S.; Rastelli, G.; Romasco, T.; Velasco-Ortega, E.; Jimenez-Guerra, A.; Iezzi, G.; Piattelli, A.; et al. Electron Microscopy (EM) Analysis of Collagen Fibers in the Peri-Implant Soft Tissues around Two Different Abutments. *J. Funct. Biomater.* **2023**, *14*, 445. https://doi.org/10.3390/jfb14090445

Academic Editor: Sergio Scombatti De Souza

Received: 21 June 2023
Revised: 25 August 2023
Accepted: 28 August 2023
Published: 29 August 2023

1. Introduction

The long-term success rate of implants depends on many factors, such as the accurate ex ante assessment of the patient's local and systemic risk factors, the ideal implant positioning, the implant macro-geometry, the prosthetic rehabilitation, and the implant maintenance [1,2]. In addition to that, the peri-implant mucosal attachment, as well as acting as a physical barrier between the oral cavity and the osseous support of the implant,

plays a key role in the prevention of microbiological infiltrations and inflammatory peri-implant diseases and contributes to the implant long-term success and survival [3]. Indeed, well-organized connective tissues around the implant were hypothesized to decrease early bone resorption by reducing inflammatory cell infiltration [4]. Accordingly, poor quality and quantity of peri-implant soft tissue could be associated with increased prosthetic failure over a long-term period [5]. Therefore, both the integrity of the epithelial lining and the health of the supra-crestal connective tissue are required to maintain implant health for a long time [6,7]. In 1996, it was established that mucosal thickness plays a crucial role in maintaining marginal bone stability, demonstrating that if the minimal requirement for the supracrestal tissue attachment (previously defined as biological width) [8], which includes a sufficient surface for both junctional epithelium and connective tissue attachments, is not met, bone resorption will take place [9]. After implant insertion, the healing period required for the formation and maturation of the supracrestal tissue attachment may last 6 to 12 weeks [10]. Even though the peri-implant soft tissue is created in response to surgical trauma or the implantation of a medical device, its dimension and composition have been constantly reported in different human histological studies [11]. On average, the supracrestal tissue attachment around implants including both the epithelial and the connective tissues measured as 3 to 4.5 mm [12].

Moreover, documenting the topography and the morphological properties of collagen fibers present around the implant neck could be essential to understanding how alterations in direction, periodicity, and diameter of collagen fibers could affect the biomechanical behavior of the peri-implant mucosa. Classical histological studies have described the arrangement of connective tissue fibers around implants in dogs and humans, attesting to the presence of parallel to long-axis, circular or ring-shaped, or inserted fibers [9,13]. Otherwise, other animal studies have described the presence of radial fibers, resembling dentogingival ones, especially around porous abutment surfaces [14].

Certain prosthetic abutments that underwent surface modifications have been able to generate a more robust and perpendicular connection between collagen fibers and the abutment. Notably, the presence of micro-grooves on implant collars produced using lasers proved high efficacy in promoting a seamless bond with the surrounding connective tissue on these surfaces [15]. The connection between the soft tissue and abutment surface provides a marked contrast to the migration of junctional epithelium toward the implant apex. This contrast contributes to the reduction of marginal bone loss (MBL) and leads to a substantial enhancement in the healing of both hard and soft tissues in the peri-implant area, as compared to using a machined surface. The same group [16] also reported that a laser-assisted new attachment procedure (LANAP) could induce regeneration of the periodontal tissues with the formation of cementum, periodontal ligament, and alveolar bone. These findings were supported also by Shapoff et al. [17] in a human study with the same laser microtextured abutments, in which it was reported optimal crestal bone levels, improved healing of the peri-implant soft tissues, and high tissue stability with a low depth of the sulcus.

In the literature, various factors have been reported to influence the quality and quantity of connective tissue attachment and healing around dental implants. For instance, different surface treatments, such as plasma or argon activation, air abrasion, acid etching, laser treatment, micro-grooving, and electrochemical oxidation, have been applied to achieve abutment micro-geometry and surface bio-activation [18,19], therefore influencing soft tissue morphogenesis. Additionally, a range of materials, including titanium, zirconium oxide, gold alloy, aluminum oxide, ceramics, titanium nitride, and hydroxyapatite, have been utilized for the same purpose. Notably, titanium and zirconia have demonstrated favorable soft tissue responses, while the use of gold alloy failed to establish an appropriate peri-implant soft tissue response [14,20,21]. Overall, rougher surfaces have exhibited improved peri-implant soft tissue characteristics, and it has been observed that epithelial cells adhere more effectively to metallic surfaces compared to ceramic surfaces [21].

Moreover, the abutment design was also demonstrated to affect the peri-implant soft tissue biological response. Collagen fibers, indeed, are not predetermined, yet they depend on the local environment. Rodriguez and co-workers [22] reported that around implants with a platform-switching design, the circular orientation of collagen fibers was observed as the main arrangement in a cross-sectional view. They argued that by increasing the room for soft tissues by changing the abutment design or its transversal discrepancy with respect to the implant platform, the supracrestal connective tissue fibers would be retained in a stable coronal position.

The geometry and behavior of the pre-existing extracellular matrix (ECM) might be modulated using mechanical and geometrical cues [23]. The design features of the implant prosthesis–abutment complex have been proven to be crucial for shaping healthy and stable peri-implant soft tissues [24]. Over the years, different abutment shapes have been proposed, from scalloped, parallel-walled, and platform-switching designs to concave ones [25–27]. These latter present an inward narrowed profile that creates a macroscopic concave profile just above the implant platform [28]. Lately, several authors have suggested that the concave design provides more space for the formation of a stable blood clot, further promoting fibroblast proliferation and migration, ECM deposition and protein adsorption, granulation tissue formation, ECM remodeling, and an increased contact area between soft tissues and the abutment, all leading to greater connective tissue stability and mechanical properties [3,14,29,30]. In this regard, Rompen et al. [31] demonstrated that a concave transmucosal design determined improved soft tissue stability with respect to divergent transmucosal abutments. In animal experimental studies, instead, other authors found denser and better-organized collagen fibers with higher connective tissue attachment, as well as significantly less peri-implant bone resorption around concave abutments, also when compared with straight designs [32,33]. Nonetheless, in their animal study, Delgado-Ruiz et al. [26] reported a lower thickness of the peri-implant soft tissues around a concave geometry of the abutment.

Considering all the above, here it is hypothesized that a concave implant neck might trigger spontaneous alignment of the collagenous network, therefore affecting fibroblast polarization, migration, and fiber growth direction and arrangement. To confirm this hypothesis, it was decided to perform a proof-of-principle animal study to study the structure and distribution of collagen fibers and bundles in the peri-implant soft tissues by comparing two implants with identical bodies but different healing abutment geometries: Test 1 presented a 2 mm concave area above the implant platform, chosen according to the positive results reported in a histological animal study and a clinical study with a similar concave profile [3,31], whereas the Control abutment had a parallel-walled healing screw.

2. Materials and Methods

2.1. Implant Characteristics

All implants were tapered shaped (IK Internal Hexagon, RESISTA® Company, Ing. Carlo Alberto Issoglio and C. S.r.l., Omegna, Italy). Test abutments (TEST) presented a 2 mm height concave portion with a double acid-etched (DAE) surface, whereas Control ones (CTRL) were parallel-walled shaped with a DAE surface. Both presented a 4 mm diameter switching platform and a length of 10 mm (Figure 1).

2.2. Ethical Statement

This animal study was approved by the Animal Ethical Committee of the Junta de Andalucia, Consejeria de Agricultura, Ganaderia, Pesca y Desarollo Sostenible on 14 December 2021 (n° 29/11/2021/184). The animal study and procedures were performed in accordance with Spain's animal protection laws and according to the Animal Research: Reporting of in Vivo Experiments (ARRIVE) guidelines [34] in a randomized prospective design.

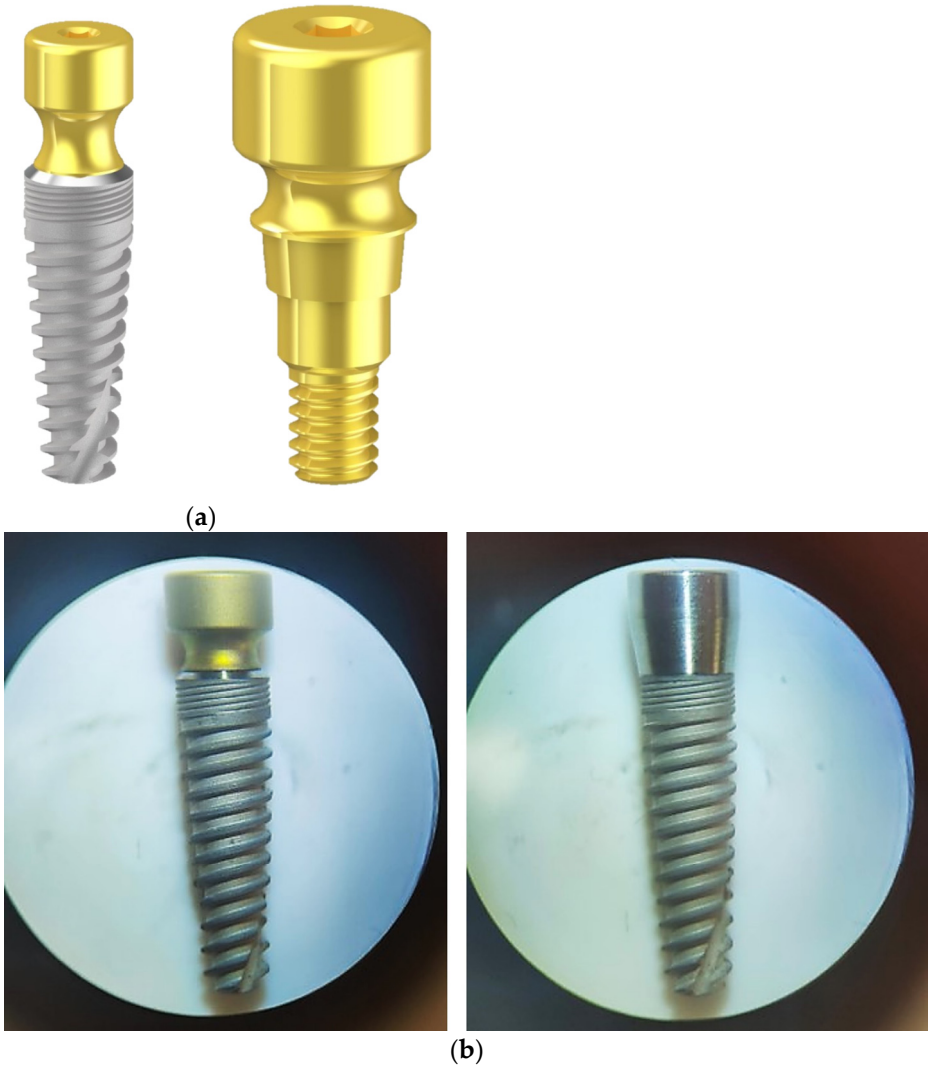

Figure 1. (**a**) Test implant and abutment (TEST); (**b**) Optical microscopy images of TEST implant (on the left) and Control implant (CTRL, on the right).

2.3. Experimental Animals and Housing

Two swine (sus scrofa), aged on average three years old, were acclimated for three weeks before the initiation of the study. The two animals were identified using an ear tag. An antibiotic-free diet, softened by soaking in water, was provided. Water was available ad libitum. The person in charge of animal welfare took care of aeration and food and water administration, as well as animal behavioral and health conditions throughout the study period. The whole study was accompanied and monitored by a veterinarian, and surgeons with extensive experience performed all surgical procedures.

2.4. Experimental Design

Animals had implants placed in the left or right mandibular alveolar ridges. Implants were either placed in the physiologically mature bone present between the lower canine and first premolar or at the mandibular premolar area, within tooth extraction sites. All implants received a healing abutment at the time of placement and 12 weeks of healing were allowed. Each animal received 6 implants, 3 per hemimandible. Control and Test implants were positioned across the jaw in a symmetrical and well-controlled manner. A total of 12 weeks after the implant placement, all animals were euthanized. Therefore, a total of 12 implants were placed. Two CTRL implants and two TEST implants were

excluded from further analysis because of early implant failure. In the end, a total of 8 implants were analyzed (CTRL, n = 4 and TEST, n = 4).

2.5. Surgical and Terminal Procedures

Before surgical intervention, animals were fasted overnight and weighed. On the day of surgery, all animals were anesthetized with intramuscular (IM) medetomidina 0.05 mg/kg + Zoletil (zolacepam + tiletamina) 3 mg/kg.

After that, a mask inhalation of 2–5% of Isoflurane mixed with oxygen was administered. Animals were transferred to the surgical area and intubated with an endotracheal tube, after which general anesthesia continued with 2–5% of Isoflurane. Monitoring of heart rate, blood oxygen saturation, and blood pressure occurred during the entirety of the procedures, as well as the post-operative period.

All surgical procedures were performed under aseptic conditions in an animal operating theater under general anesthesia. Tooth extraction was carefully completed: for all teeth, gentle pressure was applied to the gingival sulcus using a small periosteal elevator, after which mandibular premolars and molars were sectioned in a buccolingual direction at the furcation between the mesial and distal root. A rotary instrument was used for sectioning; then, a straight elevator was used to confirm sectioning. After that, the mesial and distal roots were elevated and removed using dental forceps.

In mature sites, a No. 15c blade was used to create a midcrestal incision in the area between the canine and the first premolar. A full-thickness mucoperiosteal flap was elevated and implants were placed at least 1.5 mm apart from the neighboring teeth and housed within the buccal and lingual plates using manufacturer guidelines for drilling protocol. Healing abutments were placed, and the site was closed with 4–0 silk sutures. All implants were placed equicrestally, and no bone graft was placed.

Within the first days after surgery, all animals were monitored routinely, and further analgesia was given if necessary. Post-operative surgical pain was relieved using 0.12–0.24 mg/kg buprenorphine HCl, administered subcutaneously (SC). Animals were sacrificed 12 weeks after surgery. Following sedation using the aforementioned agents, cardiac arrest was induced by administration of 110 mg/kg Pentobarbital intravenously (IV) at each previously mentioned timepoint.

2.6. Samples Preparation

Block sections were retrieved using an oscillating autopsy saw to keep the soft tissue intact. Samples of peri-implant soft tissues for histological analysis were fixed by immersion in 10% buffered formalin, dehydrated in increasing series of alcoholic rinses, and finally embedded in glycol-methacrylate resin (Technovit 7200 VLC, Wehrheim, Germany). The specimens were processed according to the protocol described in a previous study by Iezzi and collaborators [35]. Briefly, they were sectioned along its longitudinal axis to obtain histological longitudinal sections of the peri-implant tissues. Histological analysis was carried out under a light microscope (Laborlux S, Wetzlar, Germany) connected to a high-resolution video camera (3CCD, JVCKY-F55B, JVC, Yokohama, Japan) and interfaced with a PC.

Samples of peri-implant soft tissues for TEM analysis, instead, were preserved in 3.5% glutaraldehyde in 0.1 M sodium cacodylate (NaCaCO) buffer.

2.7. Electron Microscopy (EM)

2.7.1. Preparation and Analysis of Samples for EM

All implants and associated adjacent peri-implant soft tissues were removed from the mandible of each swine. Four specimens were retrieved around parallel-walled abutments (CTRL) and four specimens around concave abutments (TEST) and fixed at room temperature (RT) with 3.5% glutaraldehyde in 0.1 M NaCaCO buffer (pH 7.2) and stored at 4 °C in the fixative until shipment. Small portions of fixed soft tissues carefully dissected from the area around the implant were rinsed in 0.1 M NaCaCO buffer and then, post-fixed 2%

osmium tetroxide (OsO_4) in the same buffer for 1 h, block-stained with saturated uranyl acetate, rapidly dehydrated in graded ethanol and acetone, and embedded in epoxy resin (Epon 812) [36]. For electron microscopy (EM), ultrathin sections (~40 nm) were cut in a Leica Ultracut R microtome (Leica Microsystem, Wetzlar, Germany), using a Diatome diamond knife (Diatome Ltd., Biel, Switzerland), and after double staining with uranyl acetate and lead citrate, they were examined at 60 kV with an FP 505 Morgagni Series 268D electron microscope (FEI Company, Brno, Czech Republic), equipped with a Megaview III digital camera (Olympus, Tokyo, Japan) and Soft Imaging System (GmbH, Munster, Germany).

2.7.2. EM Ultrastructural Analysis of Collagen Bundles

For EM qualitative and quantitative analysis small samples were taken from a ring of tissue dissected all around the area of the abutment. The ultrastructural analysis of collagen from peri-implant soft tissues was mostly performed in images showing the cross-sectional appearance of the collagen fibers. Only sample regions near the abutment surface (CTRL, n = 4 and TEST, n = 4) were observed.

2.7.3. EM Quantitative Analysis of Collagen Bundles

For quantitative analysis, 15 micrographs/group were randomly collected from non-overlapping regions at 7100× of magnification and used for the following quantitative analysis:

(i) In each micrograph, the total area covered by collagen bundles was evaluated by drawing the outline of each bundle using the Soft Imaging System (GmbH, Muenster, Germany). All measured bundle values were then mathematically summarized. Only cross-sectioned bundles with a minimum size of 0.5 μm^2, where collagen fibers were distinguishable and not longitudinally oriented, were considered for the analysis. Considering that each micrograph at 7100× of magnification covers 142.6 μm^2 of sample, the relative presence of collagen bundles (%) in each sample was obtained by dividing the number of total outlined collagen fibers (in μm^2) by the total area of analyzed samples (i.e., 142.6 μm^2 × 15 micrographs).

(ii) In each micrograph, the number of longitudinally oriented bundles of collagen (of different sizes) was counted and reported as mean ± standard error of the mean (SEM) in 100 μm^2.

2.8. Statistical Analysis

In all comparisons performed between CTRL and TEST conditions, not normally distributed data were found and analyzed using a non-parametric *t*-test (Mann–Whitney test). The experimental values were elaborated using the statistical software package GraphPad Prism Software Analysis version 9.0 (San Diego, CA, USA), and the statistical significance of the differences between the groups was determined for a $p < 0.05$. Data were expressed as the mean ± SEM or standard deviation (SD).

3. Results

3.1. Radiographic Analysis

After 12 weeks, proper histologic healing was observed around both CTRL and TEST implants (Figure 2). The radiographic exams also revealed a good osseointegration of implants.

3.2. Histological Analysis

For histological analysis, transversal undecalcified sections were obtained. Histological results (Figure 3) showed the presence of peri-implant soft tissues in close connection with both TEST and CTRL abutments. However, although this is only a qualitative finding, the soft tissue appears more adherent to the concave abutment than the straight one.

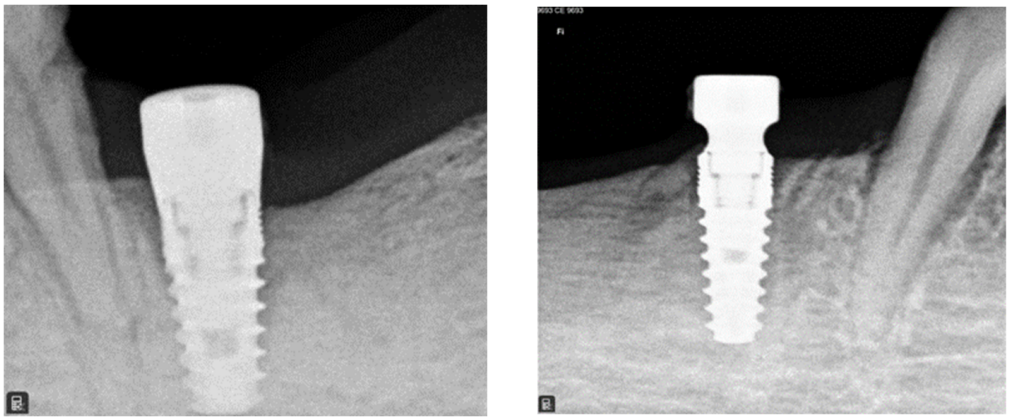

Figure 2. Representative intraoral radiographs presenting two implants placed in extractive sites of two premolars at the 3-month follow-up visit. A CTRL implant with a parallel-walled abutment on the left, and a TEST implant with a concave abutment on the right.

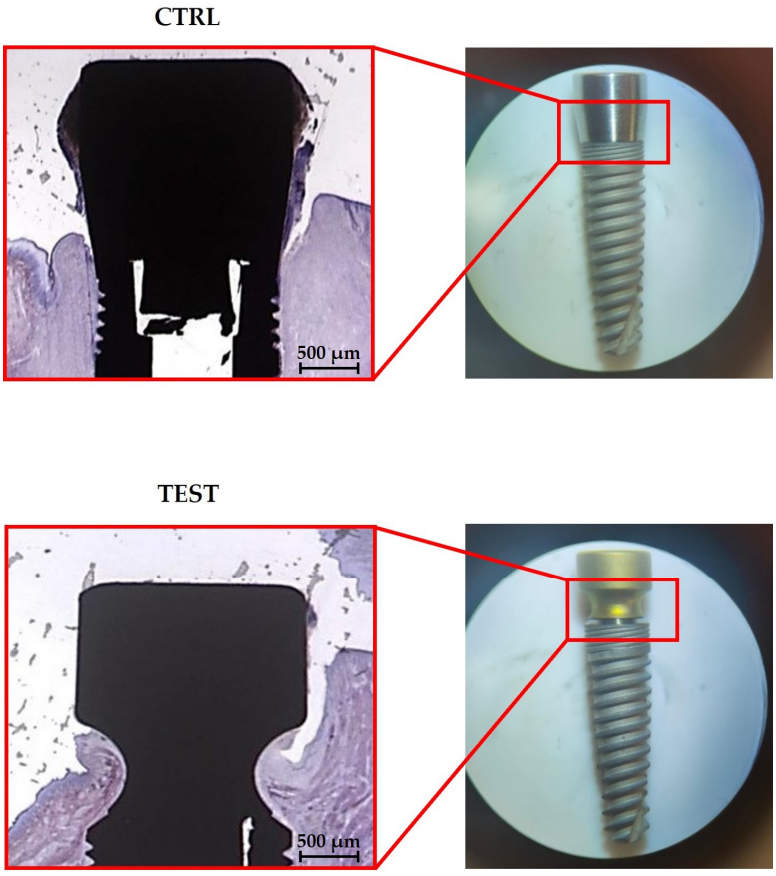

Figure 3. Histological longitudinal sections of the implant–abutment units. In the upper part, soft tissues surround the CTRL abutment. In the lower part, soft tissues surround the TEST abutment. (Acid fuchsin-Toluidine blue 20×).

3.3. EM UltrasStructural Analysis of Collagen Fibers in the Peri-Implant Soft Tissue

Ultrastructural analysis of the peri-implant soft tissue taken from sites near the two different implants (CTRL and TEST) was initially performed blinded. At the EM analysis, peri-implant soft tissues were primarily constituted by collagen fiber bundles and cells, i.e., fibroblasts (Figure 4A, f). Collagen fibers appeared as several long, parallel, and straight tubules so that when cut transversally (i.e., in cross-sectioned images), they appear as "bunches of circular spots" (Figure 4, insets), indicating bundles of heterogeneous size.

In cross-sectioned images, collagen fibers had a quite uniform diameter (0.125 nm) in both CTRL and TEST samples (Figure 4, insets).

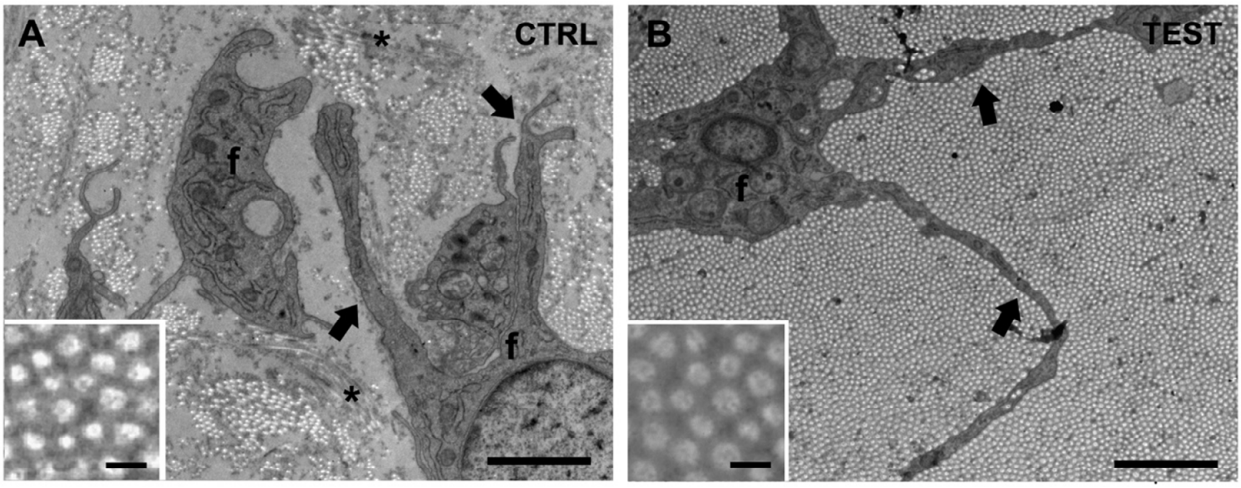

Figure 4. Representative electron microscopy (EM) images of peri-implant soft tissues around the two abutments. The peri-implant soft tissue is primarily constituted by collagen fiber bundles and fibroblasts (f); (**A**) in CTRL samples, only a few collagen fibers assembled, forming small, scattered bundles, compared to TEST samples; (**B**) in TEST samples, collagen bundles were thick and dense, often covering a large area of the analyzed section. NOTE: In the analyzed area, collagen fibers are mainly "cross-sectioned" and appear as small circles (insets), assembling in bundles of different sizes. Asterisks in panel (**A**) refer to longitudinally oriented collagen fiber bundles. Black arrows point to fibroblast processes (f). Scale bars: 2 μm; insets, 0.1 μm.

Cell populations of the peri-implant soft tissues were mostly constituted by fibroblasts (Figure 4, f), which exhibited a stellate appearance (note how fibroblast processes segregated individual collagen bundles, Figure 4, black arrows). Interestingly, during the EM analysis of the cross-sectioned collagen bundles at low magnification images (7.1k), the presence of different structural arrangements of collagen fibers between samples was quite evident. Specifically, comparing the different appearance of collagen distribution and organization allowed us to divide samples into two groups: CTRL specimens, in which an extensive aggregation of thick collagen bundles was rare or absent (Figure 4A), and TEST samples containing a high-density large aggregation of tightly packed and sorted collagen fiber bundles (Figure 4B). With more careful analysis, we also observed that in CTRL samples, there were only a few assembled collagen fibers, forming small scattered bundles, while in TEST samples, the collagen bundles were notably thick and dense, typically covering the entire area of the analyzed section (Figure 4). Specifically, in CTRL samples (Figure 4A), the collagen matrix was composed of scattered collagen bundles randomly distributed in the extracellular space at variable distances from each other. On the contrary, large areas were observed in TEST samples, where very thick collagen bundles were densely packed with each other without leaving much space for the extracellular material (Figure 4B). These data, for the first time, suggest a different growth and assembly of the collagen matrix around Test abutments when compared to Control abutments. The concave shape seemed to determine an increased bundle size of collagen fibers.

3.4. EM Quantitative Analysis of Collagen Fiber Bundles

To confirm the qualitative results, a quantitative EM analysis of images was performed (Figure 5). In detail, from cross-sectional CTRL and TEST images of the area of interest, the following features were evaluated: (i) the percentage of the total analyzed surface area covered by cross-sectioned collagen fibers (Figure 5E); (ii) the average size of the same collagen bundles (Figure 5F).

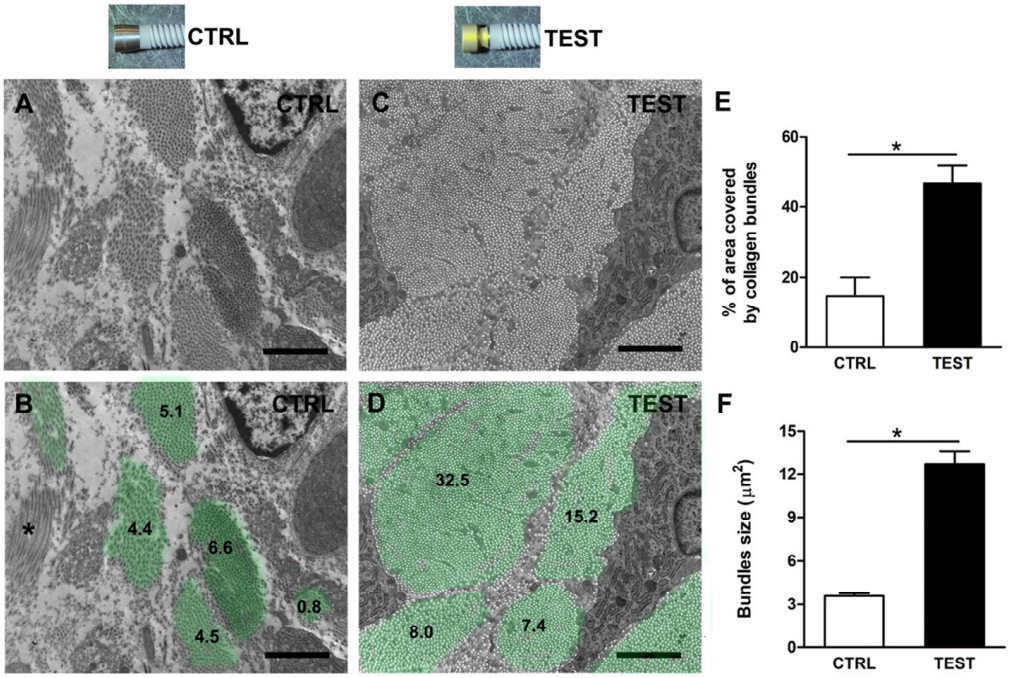

Figure 5. EM quantitative analysis of cross-sectioned collagen fiber bundles from CTRL and TEST samples. Representative EM cross-sectional images of collagen fiber bundles around (**A**) CTRL and (**C**) TEST samples, (**B**,**D**) and corresponding collagen bundles' surfaces are highlighted in light green. Numbers refer to bundles' surface areas in μm^2. Asterisk in panel (**B**) (*) refers to a longitudinal collagen fiber bundle; (**E**) Bar plot showing the quantitative analysis of the percentage of the analyzed area covered by collagen fibers; (**F**) Average size of the collagen bundles. Scale bars: 2 μm. * $p < 0.05$.

To better allow the visualization of collagen bundles' size, their surfaces have been highlighted with light green in the cross-sectional images (Figure 5B,D). The mathematical sum of each value gave a representative percentage of the surface area covered by collagen and the results have been numerically reported in Figure 5B,D. Quantitative analysis of the total surface area covered by collagen fibers indicated that the use of TEST implants was quite effective in aiding the formation and aggregation of collagen bundles in larger areas than with CTRL ones. Notably, the percentage of total surface covered by collagen was significantly higher in TEST samples (approximately 47%) with respect to CTRL ones (about 18%) (Figure 5E and Table 1).

Table 1. Percentages of the analyzed area covered by collagen bundles. Data are shown as mean ± standard deviation (SD) (* $p < 0.05$ vs CTRL).

	Sample 1	Sample 2	Sample 3	Sample 4
CTRL	18 ± 5	28 ± 3	8 ± 3	5 ± 1
TEST	47 * ± 11	46 * ± 6	63 * ± 10	43 * ± 19

Furthermore, the use of TEST abutments was also effective in significantly increasing the average size of the collagen bundles, from 4 μm^2 of the CTRL samples to 13 μm^2 (Figure 5F, Table 2, and Figure 6). The number of transversely oriented collagen bundles per 100 μm^2 was lower in TEST samples than in CTRL samples (Figure 5B,D).

Table 2. Bundles size (μm^2). Data are shown as mean ± SD (* $p < 0.05$ vs CTRL).

	Sample 1	Sample 2	Sample 3	Sample 4
CTRL	4.2 ± 5.5	4.7 ± 4.4	2.6 ± 3.8	1.5 ± 1.3
TEST	20.7 ± 27.7 *	7.5 ± 9.1	23.7 ± 12.6 *	12.6 ± 16.6 *

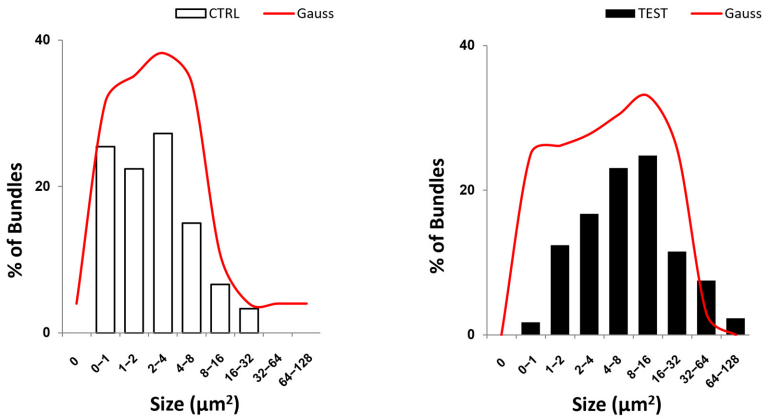

Figure 6. Representative bar and curve plots displaying the distribution frequency of bundle size for both CTRL and TEST groups. The analysis of the distribution frequency of cross-sectional area, i.e., size of bundles from CTRL and TEST groups, revealed that most bundles in the CTRL group have an average value of 3.4 ± 4.0, while in the TEST samples, the average is significantly increased to a value of 12.8 ± 16.0. This is also demonstrated by the leftward shift of the TEST frequency distribution curve compared to the CTRL curve.

3.5. Additional Ultrastructural Observations

In addition to the qualitative and quantitative differences described so far, other distinctions have been found between CTRL and TEST specimens. Indeed, it was possible to note the presence of areas characterized by abrupt changes in collagen bundle direction. In cross-sectional images of peri-implant soft tissues, collagen fibers usually appeared as small circles closely assembled in bundles of heterogeneous sizes (Figures 4 and 5). However, the presence of collagen bundles with longitudinally oriented fibers was occasionally observed (Figure 7).

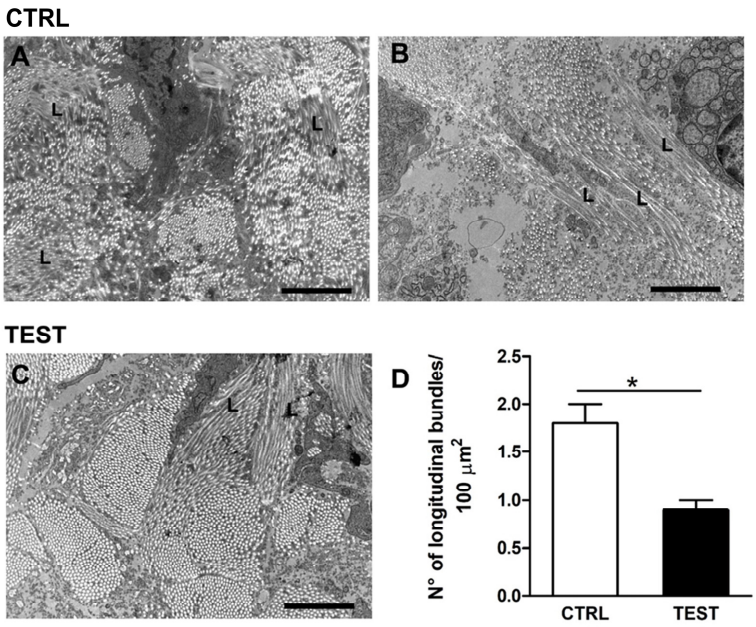

Figure 7. Representative EM images of different collagen fibers' orientation and relative quantification in (**A**,**B**) CTRL and (**C**) TEST samples. In peri-implant cross-sectioned soft tissue of the analyzed areas, collagen fibers mostly appeared as described in Figure 4, i.e., as delimited circular spots of different sizes. Occasionally, but more frequently in CTRL than in TEST samples, a longitudinal orientation of collagen fibers (L) was present; (**D**) Bar plot showing the average number of longitudinal fiber bundles per 100 µm^2 in CTRL and TEST samples. Scale bars: 2 µm. * $p < 0.05$.

After a careful examination of the specimens, longitudinally oriented fibers appeared different between CTRL and TEST samples (Figure 7). In particular, in CTRL specimens (Figure 7A,B), longitudinally oriented collagen fibers (L) are usually assembled in small-sized bundles and involve collagen fibers with a quite random orientation between each other. In TEST specimens, instead, longitudinally oriented collagen fibers (L) are assembled in larger bundles involving several, straight, and parallel-oriented fibers (Figure 7C). The number of longitudinally oriented collagen bundles per 100 μm^2 was quantified, and indeed it was found that in CTRL samples their incidence was significantly higher than in TEST samples (Table 3).

Table 3. Number of longitudinal bundles/100 μm^2. Data are shown as mean ± SEM (* $p < 0.05$ vs. CTRL).

	Sample 1	Sample 2	Sample 3	Sample 4
CTRL	1.2 ± 0.3	0.9 ± 0.2	3.4 ± 0.4	1.7 ± 0.2
TEST	1.1 ± 0.2	0.8 ± 0.2	1.1 ± 0.3 *	0.5 ± 0.2 *

4. Discussion

The present study aimed to compare the peri-implant soft tissue healing process around non-submerged implants with a parallel-walled abutment or with a concave abutment inserted in a swine model.

In a study conducted by Berglundh and Lindhe in 1996 on an animal model [9], they revealed that a specific level of mucosal thickness is essential for the formation of the supracrestal tissue attachment around dental implants. In the case of deficiency, crestal bone resorption will take place until enough space is created to accommodate both connective tissue and junctional epithelium. Despite their similarity in composition and structure, research has indicated that this attachment apparatus is longer around dental implants when compared to natural dentition, therefore necessitating a greater amount of soft tissue height around implant fixtures [13,37,38].

During recent years, several animal and human reports have described the characteristics, arrangement, and structure of peri-implant soft tissues using different techniques such as light microscopy, polarized light microscopy, scanning electron microscopy (SEM), TEM, and high-resolution X-ray phase-contrast micro-topography (XPCT) [14,26,35,39]. As an example, in two animal studies performed more than 30 years ago in monkeys [14,40], it was found that large collagen fiber bundles ran around the implant collar in a parallel way, according to a tangential circular arrangement and converging to form a "circular ring". TEM findings further showed that these circular fibers appeared to be constituted by bundles of parallel collagen fibrils with a mean diameter of 90 nm, but the inner bundles running close to the metal surface presented a less regular arrangement; indeed, they had a random course, as well as thinner and different diameters with a mean of 45 nm. Contrarily, Iezzi et al. in 2021 [35] showed transverse and longitudinal intertwined collagen bundles in a high-resolution XPCT study of peri-implant tissues around human retrieved implants. When evaluating the longitudinal sections, it was found that the closer the fiber bundles were to the metal surface, the more symmetric and regular their direction was. On the other hand, when analyzing transverse bundles of collagen fibers, it was seen a semicircular direction of these bundles, so fibers ran around the abutment, following its circular profile. Similar results were also reported by other researchers. For instance, in an animal study conducted by Bolle et al. [41], it was found that collagen fibers ran medially toward the healing abutment in a perpendicular direction and the connective tissue was dense, rich in fibroblasts and collagen fibers, which were parallel to the implant surface. Other swine studies [42] reported that in some areas, the connective tissue was well organized, while in others, the fibers exhibited a lack of organization, displaying an ambiguous and indistinct orientation. Furthermore, in human studies [35], a three-dimensional (3D) network of collagen fibers was reported around Cone–Morse implant connections. Similar results were

reported by Mangano et al. [43] using the polarized light and SEM. Collagen fibers were oriented perpendicularly up to a distance of 100 µm from the implant surface, where they became a dense and chaotic 3D network of parallel fibers running in different directions and an intimate contact of the fibrous matrix with the implant surface was found. After maturation, peri-implant connective tissue had scarce cellularity and blood vessels but became rich in collagen fibers with a few scattered fibroblasts [14].

This structure of the connective tissue has been reported to play a relevant role in the prevention of epithelium down growth and in offering mechanical protection to the osseointegrated part of the implant [35]. Also, the dense 3D framework of the connective tissue bundles determines the mechanical resistance of soft tissues to withstand forces produced during chewing [44]. There is a significant correlation between the degree of fiber orientation in the tissue and its mechanical parameters, such as the elastic modulus.

The present results demonstrated that the introduction of a concave profile in the abutment could lead to the organization of a strong wire-shaped connective tissue cuff (about 0.5 mm of thickness) over the implant platform, in which cells, fibrils, and left ECM presented a high degree of anisotropy. In this way, it has been shown how it is possible to modulate dimensions and the quality of fibers, as well as the morphogenesis of a highly aligned capillary-like network, by controlling the spatial organization of the neo-formed ECM. Taken together, these data suggested that during ECM maturation around the abutment interface, the local microenvironment could be influenced by the macroscale tissue geometry, which may trigger long-range signals by inducing internal gradients of mechanical cues, as already reported in the literature [23]. Therefore, tissue geometry acts as both a template and an instructive cue for further morphogenesis. In the present study, the CTRL group with a parallel-walled neck showed a significantly greater ratio of randomly distributed fibers. However, it is well known that moderate crosslinking is beneficial to the mechanical properties of collagen fibers, but excessive crosslinking leads collagen fibers to become more fragile [45]. In the TEST concave group, instead, collagen fibers appeared to be organized in abundant parallel bundles when seen in a section and so running circumferentially around the implant when seen from above/axial planes. This result is in line with previous literature describing collagen fiber orientation around implants with a switching platform interface, considered to be an additional "mechanical retention factor" for periodontal fiber orientation [22,25] Similarly, studies conducted on other animal models, including monkeys and dogs, have shown a supracrestal circular collagen fiber network that is even comparable to gingival ligaments [14,22].

Overall, it can be argued that the mechanical environment could play an extremely important role in collagen fiber orientation. It is believed that this phenomenon is caused by an uneven surface shear that gradually attenuated its effect with the distance [46]. The geometry of the artificial substrate might provide contact guidance for the formation of a highly polarized capillary-like network, suggesting clinical applications in triggering fast angiogenesis and perfusion in wounded tissues around the implant [47]. Specifically, collagen fibers can remodel into aligned, anisotropic ensembles under mechanical stimuli, orienting fibers into the direction of the highest applied strain. Specifically, collagen self-assembly is an entropy-driven process caused by the loss of water between monomers [48]. The goal of the mechanics-mediated fiber orientation experiments is not to recombine the collagen monomer by overcoming the interaction between monomers but to impose additional external forces on the interacting collagen monomer based on the intermolecular interaction, which can lead monomers to bond along the force direction. It can be speculated that, when the distal part of fibers meets the curve perimeter of the abutment concavity, the cellular contraction can generate sufficient force to trigger the aggregation of fibers into bundles.

Other authors believed that the organization of collagen fibers would be mainly dependent on function, namely implant loading [49]. This would lead to the interpretation of radial fibers as a circular ligament around implants. Also, the same authors have demonstrated that this collagen cuff appears to be linked to the periosteum by means

of oblique bundles. However, there are no time-dependent studies demonstrating this assumption, nor studies assessing the arrangement of collagen in different rehabilitation designs. In addition, one hypothesis would not exclude the other and vice versa.

It must be remarked that collagen is a well-engineered molecule with native weak points that represent the binding sites for metalloproteinases (MMPs) and bacterial collagenases, a mechanism favoring the regulation of collagen reshaping upon precise stimuli. It has been demonstrated that strain and external loading on fibrils could reinforce collagen in the direction of loading and inhibit the spontaneous formation of entry points for MMPs, therefore limiting their accessibility and collagen degradation [50]. It follows that directionality and immediate tension on the early wound around implants might control collagen assembly and maturation. Many human tissues are featured by specific alignment patterns involving the ECM of the interstitial connective tissue, stromal cells, and vascular network [51]. Collagen arranged in bundles of aligned fibers controls not only the mechanical properties of tissues, but its density and alignment direction also triggers the polarization of several biological phenomena: cell migration, morphogenesis, vascularization, innervation, tissue regeneration, and wound healing [52]. In any case, having the possibility to control the alignment of a fibroblast-synthetized ECM network still represents a challenge in dentistry.

5. Conclusions

In conclusion, within the limitations of the present study due to the use of a small number of animals and implants that might bring uncertainty and risk to the research results, the present study on the peri-implant connective tissue structure evaluated by histological and TEM analysis showed that the concave transmucosal design could favor the deposition and growth of the connective tissue. This concavity generated a significant amount of connective tissue in the early healing phase, increased the thickness of this circular peri-implant network, and promoted the convergence of collagen fibers toward the abutment collar with the formation of a wide circular collagen structure over the implant platform.

Therefore, starting from our proof-of-principle animal study, future research involving a larger number of animals and implants, as well as using other mechanical detection methods together with histological and TEM analysis, will be necessary to confirm and strengthen the present results.

Author Contributions: Conceptualization, U.C., A.P. and S.M.; methodology, E.G., S.B., G.R., T.R., E.V.-O., A.J.-G. and G.I.; software, S.B. and T.R.; validation, N.D.P., G.I. and A.P.; formal analysis, T.R., G.R. and E.G.; investigation, A.J.-G., E.V.-O., S.B. and G.I.; resources, U.C. and A.P.; data curation, N.D.P. and S.M.; writing—original draft preparation, N.D.P., T.R., E.G, S.M., S.B. and A.P.; writing—review and editing, N.D.P. and T.R.; visualization, G.I. and S.M.; supervision, U.C. and A.P.; project administration, U.C. and S.M. All authors have read and agreed to the published version of the manuscript.

Funding: This research received no external funding.

Institutional Review Board Statement: The animal study protocol was approved by the Animal Ethical Committee of JUNTA DE ANDALUCIA, CONSEJERIA DE AGRICULTURA, GANDERIA, PESCA Y DESAROLLO SOSTENIBLE (protocol code 29/11/2021/184, 14 December 2021).

Informed Consent Statement: Not applicable.

Data Availability Statement: Data are contained within the article and available on request from the corresponding author. The data are not publicly available due to privacy.

Acknowledgments: The authors would like to acknowledge RESISTA® Company, Ing. Carlo Alberto Issoglio, and C. S.r.l., Omegna, Italy for providing implants at no cost.

Conflicts of Interest: The authors declare no conflict of interest.

References

1. Albrektsson, T.; Brånemark, P.I.; Hansson, H.A.; Lindström, J. Osseointegrated Titanium Implants. Requirements for Ensuring a Long-Lasting, Direct Bone-to-Implant Anchorage in Man. *Acta Orthop. Scand.* **1981**, *52*, 155–170. [CrossRef] [PubMed]
2. Geckili, O.; Bilhan, H.; Geckili, E.; Cilingir, A.; Mumcu, E.; Bural, C. Evaluation of Possible Prognostic Factors for the Success, Survival, and Failure of Dental Implants. *Implant Dent.* **2014**, *23*, 44–50. [CrossRef]
3. Bolle, C.; Gustin, M.P.; Fau, D.; Exbrayat, P.; Boivin, G.; Grosgogeat, B. Early Periimplant Tissue Healing on 1-Piece Implants with a Concave Transmucosal Design: A Histomorphometric Study in Dogs. *Implant Dent.* **2015**, *24*, 598–606. [CrossRef] [PubMed]
4. Lindhe, J.; Meyle, J.; on behalf of Group D of the European Workshop on Periodontology. Peri-implant diseases: Consensus Report of the Sixth European Workshop on Periodontology. *J. Clin. Periodontol.* **2008**, *35*, 282–285. [CrossRef]
5. Schwarz, F.; Ramanauskaite, A. It Is All about Peri-Implant Tissue Health. *Periodontology 2000* **2022**, *88*, 9–12. [CrossRef]
6. Suárez-López del Amo, F.; Lin, G.-H.; Monje, A.; Galindo-Moreno, P.; Wang, H.-L. Influence of Soft Tissue Thickness on Peri-Implant Marginal Bone Loss: A Systematic Review and Meta-Analysis. *J. Periodontol.* **2016**, *87*, 690–699. [CrossRef] [PubMed]
7. Ivanovski, S.; Lee, R. Comparison of Peri-Implant and Periodontal Marginal Soft Tissues in Health and Disease. *Periodontology 2000* **2018**, *76*, 116–130. [CrossRef]
8. Jepsen, S.; Caton, J.G.; Albandar, J.M.; Bissada, N.F.; Bouchard, P.; Cortellini, P.; Demirel, K.; de Sanctis, M.; Ercoli, C.; Fan, J.; et al. Periodontal manifestations of systemic diseases and developmental and acquired conditions: Consensus report of workgroup 3 of the 2017 World Workshop on the Classification of Periodontal and Peri-Implant Diseases and Conditions. *J. Periodontol.* **2018**, *89* (Suppl. 1), S237–S248. [CrossRef] [PubMed]
9. Berglundh, T.; Lindhe, J. Dimension of the Periimplant Mucosa. Biological Width Revisited. *J. Clin. Periodontol.* **1996**, *23*, 971–973. [CrossRef]
10. Berglundh, T.; Abrahamsson, I.; Welander, M.; Lang, N.P.; Lindhe, J. Morphogenesis of the Peri-Implant Mucosa: An Experimental Study in Dogs. *Clin. Oral Implant. Res.* **2007**, *18*, 1–8. [CrossRef]
11. Mattheos, N.; Janda, M.; Acharya, A.; Pekarski, S.; Larsson, C. Impact of Design Elements of the Implant Supracrestal Complex (ISC) on the Risk of Peri-Implant Mucositis and Peri-Implantitis: A Critical Review. *Clin. Oral Implant. Res.* **2021**, *32* (Suppl. 21), 181–202. [CrossRef] [PubMed]
12. Glauser, R.; Schüpbach, P.; Gottlow, J.; Hämmerle, C.H.F. Periimplant Soft Tissue Barrier at Experimental One-Piece Mini-Implants with Different Surface Topography in Humans: A Light-Microscopic Overview and Histometric Analysis. *Clin. Implant Dent. Relat. Res.* **2005**, *7* (Suppl. 1), s44–s51. [CrossRef]
13. Abrahamsson, I.; Berglundh, T.; Wennström, J.; Lindhe, J. The Peri-Implant Hard and Soft Tissues at Different Implant Systems. A Comparative Study in the Dog. *Clin. Oral Implant. Res.* **1996**, *7*, 212–219. [CrossRef]
14. Ruggeri, A.; Franchi, M.; Marini, N.; Trisi, P.; Piattelli, A. Supracrestal Circular Collagen Fiber Network around Osseointegrated Nonsubmerged Titanium Implants. *Clin. Oral Implant. Res.* **1992**, *3*, 169–175. [CrossRef] [PubMed]
15. Nevins, M.; Kim, D.K.; Jun, S.H.; Guze, K.; Schupbach, P.; Nevins, M.L. Histologic evidence of a connective tissue attachment to laser microgrooved abutments: A canine study. *Int. J. Periodontics Restor. Dent.* **2010**, *30*, 245–255.
16. Nevins, M.L.; Camelo, M.; Schupbach, P.; Kim, S.W.; Kim, D.M.; Nevins, M. Human clinical and histologic evaluation of laser-assisted new attachment procedure. *Int. J. Periodontics Restor. Dent.* **2012**, *32*, 497–507.
17. Shapoff, C.A.; Babushkin, J.A.; Wohl, D.J. Clinical Use of Laser-Microtextured Abutments: A Case Series. *Int. J. Periodontics Restor. Dent.* **2016**, *39*, 655–662. [CrossRef]
18. Pesce, P.; Menini, M.; Tommasato, G.; Patini, R.; Canullo, L. Influence of modified titanium abutment surface on peri-implant soft tissue behaviour: A systematic review of histological findings. *Int. J. Oral Implantol.* **2019**, *12*, 419–429.
19. Geurs, N.C.; Geisinger, M.L.; Vassilopoulos, P.J.; O'Neal, S.J.; Haigh, S.J.; Reddy, M.S. Optimizing Connective Tissue Integration on Laser-Ablated Implant Abutments. *Clin. Adv. Periodontics* **2016**, *6*, 153–159. [CrossRef]
20. Roehling, S.; Schlegel, K.A.; Woelfler, H.; Gahlert, M. Zirconia compared to titanium dental implants in preclinical studies-A systematic review and meta-analysis. *Clin. Oral Implant. Res.* **2019**, *30*, 365–395. [CrossRef]
21. Blázquez-Hinarejos, M.; Ayuso-Montero, R.; Jané-Salas, E.; López-López, J. Influence of surface modified dental implant abutments on connective tissue attachment: A systematic review. *Arch. Oral Biol.* **2017**, *80*, 185–192. [CrossRef] [PubMed]
22. Rodríguez, X.; Vela, X.; Calvo-Guirado, J.L.; Nart, J.; Stappert, C.F.J. Effect of Platform Switching on Collagen Fiber Orientation and Bone Resorption around Dental Implants: A Preliminary Histologic Animal Study. *Int. J. Oral Maxillofac. Implant.* **2012**, *27*, 1116–1122.
23. Nelson, C.M. Geometric Control of Tissue Morphogenesis. *Biochim. Biophys. Acta* **2009**, *1793*, 903–910. [CrossRef]
24. Mattheos, N.; Vergoullis, I.; Janda, M.; Miseli, A. The Implant Supracrestal Complex and Its Significance for Long-Term Successful Clinical Outcomes. *Int. J. Prosthodont.* **2021**, *34*, 88–100. [CrossRef]
25. Ciurana, X.; Acedo, Á.; Vela, X.; Fortuño, A.; García, J.; Nevins, M. Arrangement of Peri-Implant Connective Tissue Fibers Around Platform-Switching Implants with Conical Abutments and Its Relationship to the Underlying Bone: A Human Histologic Study. *Int. J. Periodontics Restor. Dent.* **2016**, *36*, 533–540. [CrossRef] [PubMed]
26. Delgado-Ruiz, R.A.; Calvo-Guirado, J.L.; Abboud, M.; Ramirez-Fernandez, M.P.; Maté-Sánchez de Val, J.E.; Negri, B.; Gomez-Moreno, G.; Markovic, A. Connective Tissue Characteristics around Healing Abutments of Different Geometries: New Methodological Technique under Circularly Polarized Light. *Clin. Implant Dent. Relat. Res.* **2015**, *17*, 667–680. [CrossRef]

27. Kim, S.; Oh, K.C.; Han, D.H.; Heo, S.J.; Ryu, I.C.; Kwon, J.H.; Han, C.H. Influence of transmucosal designs of three one-piece implant systems on early tissue responses: A histometric study in beagle dogs. *Int. J. Oral Maxillofac. Implant.* **2010**, *25*, 309–314.
28. Bishti, S.; Strub, J.R.; Att, W. Effect of the Implant-Abutment Interface on Peri-Implant Tissues: A Systematic Review. *Acta Odontol. Scand.* **2014**, *72*, 13–25. [CrossRef]
29. Gibbs, S.; Roffe, S.; Meyer, M.; Gasser, A. Biology of Soft Tissue Repair: Gingival Epithelium in Wound Healing and Attachment to the Tooth and Abutment Surface. *Eur. Cells Mater.* **2019**, *38*, 63–78. [CrossRef]
30. Valente, N.; Wu, M.; Toti, P.; Derchi, G.; Barone, A. Impact of Concave/Convergent vs Parallel/Divergent Implant Transmucosal Profiles on Hard and Soft Peri-Implant Tissues: A Systematic Review with Meta-Analyses. *Int. J. Prosthodont.* **2020**, *33*, 553–564. [CrossRef]
31. Rompen, E.; Raepsaet, N.; Domken, O.; Touati, B.; Van Dooren, E. Soft Tissue Stability at the Facial Aspect of Gingivally Converging Abutments in the Esthetic Zone: A Pilot Clinical Study. *J. Prosthet. Dent.* **2007**, *97*, S119–S125. [CrossRef] [PubMed]
32. Chien, H.H.; Schroering, R.L.; Prasad, H.S.; Tatakis, D.N. Effects of a New Implant Abutment Design on Peri-Implant Soft Tissues. *J. Oral Implantol.* **2014**, *40*, 581–588. [CrossRef] [PubMed]
33. Huh, J.B.; Rheu, G.B.; Kim, Y.S.; Jeong, C.M.; Lee, J.Y.; Shin, S.W. Influence of Implant Transmucosal Design on Early Peri-Implant Tissue Responses in Beagle Dogs. *Clin. Oral Implant. Res.* **2014**, *25*, 962–968. [CrossRef] [PubMed]
34. du Sert, N.P.; Hurst, V.; Ahluwalia, A.; Alam, S.; Avey, M.T.; Baker, M.; Browne, W.J.; Clark, A.; Cuthill, I.C.; Dirnagl, U.; et al. The ARRIVE Guidelines 2.0: Updated Guidelines for Reporting Animal Research. *PLoS Biol.* **2020**, *18*, e3000410. [CrossRef]
35. Iezzi, G.; Di Lillo, F.; Furlani, M.; Degidi, M.; Piattelli, A.; Giuliani, A. The Symmetric 3d Organization of Connective Tissue around Implant Abutment: A Key-Issue to Prevent Bone Resorption. *Symmetry* **2021**, *13*, 1126. [CrossRef]
36. Boncompagni, S.; Rossi, A.E.; Micaroni, M.; Beznoussenko, G.V.; Polishchuk, R.S.; Dirksen, R.T.; Protasi, F. Mitochondria Are Linked to Calcium Stores in Striated Muscle by Developmentally Regulated Tethering Structures. *Mol. Biol. Cell* **2009**, *20*, 1058–1067. [CrossRef] [PubMed]
37. Abrahamsson, I.; Berglundh, T.; Moon, I.S.; Lindhe, J. Peri-implant tissues at submerged and non-submerged titanium implants. *J. Clin. Periodontol.* **1999**, *26*, 600–607. [CrossRef] [PubMed]
38. Berglundh, T.; Lindhe, J.; Ericsson, I.; Marinello, C.P.; Liljenberg, B.; Thomsen, P. The soft tissue barrier at implants andteeth. *Clin. Oral Implant. Res.* **1991**, *2*, 81–90. [CrossRef]
39. Giuliani, A.; Cedola, A. *Advanced High-Resolution Tomography in Regenerative Medicine*; Springer: Berlin/Heidelberg, Germany, 2018. [CrossRef]
40. Ruggeri, A.; Franchi, M.; Trisi, P.; Piattelli, A. Histologic and Ultrastructural Findings of Gingival Circular Ligament Surrounding Osseointegrated Nonsubmerged Loaded Titanium Implants. *Int. J. Oral Maxillofac. Implant.* **1994**, *9*, 636–643.
41. Bolle, C.; Gustin, M.-P.; Fau, D.; Boivin, G.; Exbrayat, P.; Grosgogeat, B. Soft Tissue and Marginal Bone Adaptation on Platform-Switched Implants with a Morse Cone Connection: A Histomorphometric Study in Dogs. *Int. J. Periodontics Restor. Dent.* **2016**, *36*, 221–228. [CrossRef]
42. Tetè, S.; Mastrangelo, F.; Bianchi, A.; Zizzari, V.; Scarano, A. Collagen Fiber Orientation around Machined Titanium and Zirconia Dental Implant Necks: An Animal Study. *Int. J. Oral Maxillofac. Implant.* **2009**, *24*, 52–58.
43. Mangano, C.; Piattelli, A.; Scarano, A.; Raspanti, M.; Shibli, J.; Mangano, F.; Perrotti, V.; Iezzi, G. A Light and Scanning Electron Microscopy Study of Human Direct Laser Metal Forming Dental Implants. *Int. J. Periodontics Restor. Dent.* **2014**, *34*, 9–17. [CrossRef]
44. Romanos, G.E.; Traini, T.; Johansson, C.B.; Piattelli, A. Biologic Width and Morphologic Characteristics of Soft Tissues around Immediately Loaded Implants: Studies Performed on Human Autopsy Specimens. *J. Periodontol.* **2010**, *81*, 70–78. [CrossRef]
45. Buehler, M.J. Nature Designs Tough Collagen: Explaining the Nanostructure of Collagen Fibrils. *Proc. Natl. Acad. Sci. USA* **2006**, *103*, 12285–12290. [CrossRef]
46. Lin, J.; Shi, Y.; Men, Y.; Wang, X.; Ye, J.; Zhang, C. Mechanical Roles in Formation of Oriented Collagen Fibers. *Tissue Eng. Part B Rev.* **2020**, *26*, 116–128. [CrossRef]
47. Casale, C.; Imparato, G.; Mazio, C.; Netti, P.A.; Urciuolo, F. Geometrical Confinement Controls Cell, ECM and Vascular Network Alignment during the Morphogenesis of 3D Bioengineered Human Connective Tissues. *Acta Biomater.* **2021**, *131*, 341–354. [CrossRef] [PubMed]
48. Sun, B. The Mechanics of Fibrillar Collagen Extracellular Matrix. *Cell Rep. Phys. Sci.* **2021**, *2*. [CrossRef]
49. Schierano, G.; Ramieri, G.; Cortese, M.G.; Aimetti, M.; Preti, G. Organization of the Connective Tissue Barrier around Long-Term Loaded Implant Abutments in Man. *Clin. Oral Implant. Res.* **2002**, *13*, 460–464. [CrossRef]
50. Birk, D.E.; Nurminskaya, M.V.; Zycband, E.I. Collagen Fibrillogenesis in Situ: Fibril Segments Undergo Post-Depositional Modifications Resulting in Linear and Lateral Growth during Matrix Development. *Dev. Dyn.* **1995**, *202*, 229–243. [CrossRef] [PubMed]

51. Yang, G.; Mahadik, B.; Choi, J.Y.; Fisher, J.P. Vascularization in Tissue Engineering: Fundamentals and State-of-Art. *Prog. Biomed. Eng.* **2020**, *2*, 012002. [CrossRef]
52. Saeidi, N.; Karmelek, K.P.; Paten, J.A.; Zareian, R.; DiMasi, E.; Ruberti, J.W. Molecular Crowding of Collagen: A Pathway to Produce Highly-Organized Collagenous Structures. *Biomaterials* **2012**, *33*, 7366–7374. [CrossRef]